

A new goniopholidid crocodylomorph from the Late Jurassic of Portugal

Víctor López-Rojas, Simão Mateus, João Marinheiro,
Octávio Mateus, and Eduardo Puértolas-Pascual

ABSTRACT

Plenty of goniopholidid species from the Mesozoic have been found in the Iberian Peninsula. A previous goniopholidid taxon, *Goniopholis baryglyphaeus* Schwarz, 2002, from the Late Jurassic of the Guimarães coal mine (Leiria, central Portugal) was described. This taxon corresponds to a partial skull and some postcranial material, and it marked the oldest and first ever record of goniopholidid and *Goniopholis* species described for the Iberian Peninsula. Here we present a well-preserved, almost complete, skull of a new species, *Ophiussasuchus paimogonectes* gen. et sp. nov. from Upper Jurassic deposits of Praia de Paimogo (near Lourinhã, central west Portugal). The specimen corresponds to a mesorostrine, platyrostral skull of a medium-sized goniopholidid coming from the upper Kimmeridgian within the Lourinhã Formation. Phylogenetically, the new species is recovered as the sister taxon of the Early Cretaceous European clade made by *Hulkepholis* and *Anteophthalmosuchus*. Although its position is well-resolved, this new taxon displays intermediate morphological traits, sharing characteristics with Jurassic Asian and American basal goniopholidids (e.g., presence but lesser development of the secondary choana with the nasopharyngeal duct partially open), as well as more derived characters shared with Cretaceous European taxa such as *Hulkepholis* (e.g., the shape of the supratemporal fenestra and the palatines). As a result, *Ophiussasuchus paimogonectes* gen. et sp. nov. exhibits characteristics suggesting a reversion to primitive goniopholidid conditions or intermediate states between the goniopholidid taxa of North America and Europe. These findings support the shared Late Jurassic fauna between the Morrison and Lourinhã Formations, while also having high endemism of taxa.

Víctor López-Rojas. Museu da Lourinhã, Rua João Luís de Moura, 95, 2530-158 Lourinhã, Portugal and GeoBioTec, Faculdade de Ciências e Tecnologia da Universidade Nova de Lisboa, 2829-516 Monte de Caparica, Portugal (correspondance author). v.rojas@campus.fct.unl.pt

<https://zoobank.org/D9A2DA25-F372-4FB4-A3EC-B1F6516534F5>

Final citation: López-Rojas, Víctor, Mateus, Simão, Marinheiro, João, Mateus, Octávio, and Puértolas-Pascual, Eduardo. 2024. A new goniopholidid crocodylomorph from the Late Jurassic of Portugal. *Palaeontologia Electronica*, 27(1):a5.

<https://doi.org/10.26879/1316>

palaeo-electronica.org/content/2024/5106-a-new-portuguese-goniopholidid

Copyright: January 2024 Paleontological Society.

This is an open access article distributed under the terms of Attribution-NonCommercial-ShareAlike 4.0 International (CC BY-NC-SA 4.0), which permits users to copy and redistribute the material in any medium or format, provided it is not used for commercial purposes and the original author and source are credited, with indications if any changes are made.
creativecommons.org/licenses/by-nc-sa/4.0/

Simão Mateus. Museu da Lourinhã, Rua João Luís de Moura, 95, 2530-158 Lourinhã, Portugal, GeoBioTec, Faculdade de Ciências e Tecnologia da Universidade Nova de Lisboa, 2829-516 Monte de Caparica, Portugal, and Parque dos Dinossauros da Lourinhã, Rua Vale dos Dinossauros, 25, Abelheira, 2530-059 Lourinhã, Portugal. simaomateus@gmail.com

João Marinheiro. Museu da Lourinhã, Rua João Luís de Moura, 95, 2530-158 Lourinhã, Portugal and Parque dos Dinossauros da Lourinhã, Rua Vale dos Dinossauros, 25, Abelheira, 2530-059 Lourinhã, Portugal. joamarinh@gmail.com

Octávio Mateus. Museu da Lourinhã, Rua João Luís de Moura, 95, 2530-158 Lourinhã, Portugal and GeoBioTec, Faculdade de Ciências e Tecnologia da Universidade Nova de Lisboa, 2829-516 Monte de Caparica, Portugal. omateus@fct.unl.pt

Eduardo Puértolas-Pascual. Museu da Lourinhã, Rua João Luís de Moura, 95, 2530-158 Lourinhã, Portugal, GeoBioTec, Faculdade de Ciências e Tecnologia da Universidade Nova de Lisboa, 2829-516 Monte de Caparica, Portugal, and Aragosaurus-IUCA Research group, Universidad de Zaragoza, C/ Pedro Cerbuna 12, 50009, Zaragoza, Spain. puertolas@unizar.es

Keywords: new genus; new species; Lourinhã Formation; upper Kimmeridgian; Crocodylomorpha; phylogeny

Submission: 6 July 2023. Acceptance: 18 December 2023.

INTRODUCTION

Portugal is well known for the diversity of dinosaur remains found in the country (Bonaparte and Mateus, 1999; Mateus, 2006; Ortega et al., 2006; Hendrickx and Mateus, 2014; Mocho et al., 2017a; Mocho et al., 2017b; Costa and Mateus, 2019; Malafaia et al., 2019; Mocho et al., 2019; Castanera et al., 2020; Mateus and Estraviz-López, 2022; Rotatori et al., 2022). However, the Portuguese crocodyliform remains are also abundant and diverse, spanning from the Jurassic until the Miocene (Schwarz and Salisbury, 2005; Puértolas-Pascual et al., 2016; Antunes, 2017; Mateus et al., 2019). From the Late Jurassic, there are findings of crocodylomorph remains consisting of bones, teeth, footprints and even eggshells (Schwarz and Fechner, 2004; Mateus and Milàn, 2010; Russo et al., 2014; Young et al., 2014; Schwarz et al., 2017; Guillaume et al., 2020; Puértolas-Pascual and Mateus, 2020). Among these crocodylomorphs, the goniopholidids were an important clade that lived in Europe by the Late Jurassic until the Early Cretaceous (Buscalioni et al., 2013; Puértolas-Pascual et al., 2016; Puértolas-Pascual and Mateus, 2020).

Goniopholididae is a well-known extinct group of neosuchian crocodyliform taxa that bear resemblance, externally in general shape and lifestyle, to extant crocodylians (Pritchard et al., 2013; Martin et al., 2016), ranking from the Early Jurassic *Calsoyasuchus valliceps*, Tykoski, Rowe, Ketcham, and Colbert, 2002 as the oldest representative, until the Late Cretaceous with *Denazinosuchus*

kirtlandicus Wiman, 1932 as the youngest representative of the clade (Sullivan and Lucas, 2003). This clade was common in the Northern Hemisphere, where fossils are mostly found in North America (Allen, 2012) and Europe (Ristevski et al., 2018), with some remains found also in Africa (Goodwin et al., 1999) and Asia (Maisch et al., 2003; Cuny et al., 2010). Despite their high resemblance with extant crocodylians, goniopholidids still retain some primitive features, such as the participation of the palatines in the choana, biserial paravertebral armor, or the amphicoelous vertebrae. At the same time, they have also developed some unique features, such as the maxillary depressions, a characteristic feature of Goniopholididae (Andrade and Hornung, 2011; Allen, 2012; Arribas et al., 2019), shared with some pholidosaurids (Martin and Buffetaut, 2012). While the exact function of the maxillary depression remains mysterious, it probably had sensorial function (Andrade, 2009).

The first potential goniopholidid described from the Iberian Peninsula was the now *nomen dubium* of *Oweniasuchus lusitanicus* (Sauvage, 1897-1898) from the Late Cretaceous (Cenomanian) of Portugal, based on a partial mandible and isolated teeth. However, the oldest goniopholidid from the Iberian Peninsula is from the Late Jurassic of the Guimarota coalmine (Portugal), *Goniopholis baryglyphaeus* Schwarz, 2002. This species was described based on a fragmentary skull and isolated postcranial remains. Another two goniopholidid genera, *Anteophthalmosuchus* and

Hulkepholis (Buscalioni et al., 2013; Puértolas-Pascual et al., 2015; Arribas et al., 2019) were described from Teruel (Spain) as being closer looking species from the same genera found in Wessex region (United Kingdom) (Salisbury and Naish, 2011; Ristevski et al., 2018) and Bernissart (Belgium) (Martin et al., 2016). These Early Cretaceous Iberian species are: *Anteophthalmosuchus escuchae* Buscalioni, Alcalá, Espílez and Mampel, 2013, a partial skeleton and a disarticulated skull, plus several isolated teeth; and *Hulkepholis plotos* Buscalioni, Alcalá, Espílez, and Mampel, 2013 and *Hulkepholis rori* Arribas, Buscalioni, Royo Torres, Espílez, Mampel, and Alcalá, 2019, also as partial skeletons and skull remains. These four Iberian species represent the oldest (*G. baryglyphaeus*) and the youngest (*Anteophthalmosuchus escuchae* and *Hulkepholis plotos*) record of goniopholidids found in the Iberian Peninsula and Europe.

Isolated goniopholidid teeth are one of the most common vertebrate fossils in the Lourinhã Fm, but too fragmentary to allow any identification to the species level (Guillaume et al., 2020). Here, we describe a new species of Goniopholididae, based on an almost complete skull from the Late Jurassic (upper Kimmeridgian-lower Tithonian) of the Lourinhã Formation (west Portugal).

GEOLOGICAL SETTINGS

The specimen studied here was recovered on the Paimogo beach, located in the Lusitanian Basin, about 7 km north of the town of Lourinhã (Lisbon, Portugal).

The rocks that are exposed at the Paimogo locality are dated to the Upper Jurassic (Kimmeridgian-Tithonian) Lourinhã Formation, and more specifically to the middle member called the Praia Azul Member (Ribeiro et al. 2014; Mateus et al. 2017). The Lourinhã Fm is a sedimentary succession characterized by alternating terrestrial marls, mudstone, and sandstone facies representing deposition in alluvial fan and fluvio-deltaic environments, with local carbonate levels that correspond to estuarine and lagoon settings (e.g., Hill, 1989; Manuppella et al., 1999; Martinius and Gowland, 2011; Myers et al., 2012; Taylor et al., 2014). This unit is worldwide known for its richness in fossil vertebrate fauna including lissamphibians, mammals and dinosaurs (Ribeiro et al., 2014). Paleoclimate reconstructions suggest semiarid and seasonal conditions during deposition of the Lourinhã Fm (Martinius and Gowland, 2011; Myers et al., 2012), and the paleolatitude was around 28-29°N based

on paleolatitude estimates available at paleolatitude.org (van Hinsbergen et al., 2015).

The Praia Azul Member is a characteristic interval of the Lourinhã Fm as it records three carbonate layers intercalated between the sandstones and marlstones bodies, which represent short transgressive phases (Ribeiro et al., 2014; Mateus et al., 2017). The lower and upper levels are used as lithostratigraphic boundaries (Manuppella et al., 1999), which can be traced over distances of 20 km and are rich in brackish faunas (Hill, 1989; Manuppella et al., 1999; Martinius and Gowland, 2011; Myers et al., 2012; Taylor et al., 2014; Mateus et al., 2017). The Praia Azul Member is known to bear abundant dinosaur remains, including bones, eggs, and tracks (Ribeiro et al., 2014), as well as crocodylomorphs, turtles, pterosaurs, mammals, lissamphibians, and lepidosaurs. The different faunal assemblages that can be found in this member include the bivalves *Eomiodon securiformes* Sharpe, 1850, *Arcomytilus morrisii* Sharpe, 1850, *Isognomon lusitanicus* Sharpe, 1850, other ostreids and dinosaur tracks in the lower carbonate level (outcropping north of Caniçal, below the Paimogo fort); the bivalves *Jurassicorbula edwardsi* Sharpe, 1850, *Isognomon lusitanica*, *Nerinea*, *Eomiodon securiformes*, coprolites, fish remains, and echinoids in the middle level (outcropping north of Paimogo, at the base of Praia do Caniçal); and the *Jurassicorbula edwardsi*, *Isognomon lusitanicus*, other abundant ostreids and pleurosternidae turtles in the upper level (outcropping at the top of Praia do Caniçal) (Ribeiro et al., 2014; Mateus et al., 2017).

The specimen of the present work was extracted from an isolated beach boulder in Praia de Paimogo. Due to the geographical conditions of the bay, surrounded by Upper Jurassic rocks forming the 50 m tall sea cliffs, the fossils must have fallen from the layers above, and been eroded by the ocean over the years. The block in which the specimen was found was a grayish sandstone like the layers seen above in the Paimogo cliffs, probably situated between the first and second carbonate layers. Based on its location, the estimated age of the specimen is around 149 million years old. Historically, the locality of Paimogo is famous for the finding of dinosaur eggs (Mateus et al., 1998; Cunha et al., 2004; Fernandes et al., 2021), although these findings correspond to the layers of the top of the underlying unit of Amoreira-Porto Novo Member. In the location where this specimen was collected are deposit outcrops of the lower half of the Praia Azul Mb. of Lourinhã Fm, below the

second marine transgression, which was dated as coinciding to the Kimmeridgian/Tithonian transition. The fossil ML2776, here studied, is therefore from the upper Kimmeridgian.

MATERIALS AND METHODS

The material was discovered in December 2021 by Holger Lütke, the same finder of *Europasaurus holgeri*. The discovery consists of a single block, rolled, without recent scars of falling apart. Mr Holger Lütke contacted Dino Park of Münchshagen (Germany) and Parque dos Dinossauros da Lourinhã (Portugal), and the block was donated to the Museum of Lourinhã through Simão Mateus. The specimen is to be housed in Museu da Lourinhã (Portugal) following current archival standards.

The specimen ML 2776 was transported to the Parque dos Dinossauros da Lourinhã and was prepared using pneumatic tools. For the removal of the surrounding matrix was used *Presslufthammer* HW 65 and HW 70. For removing the matrix closer to the fossil was used *Presslufthammer* HW 70 and HW 322. And, for the matrix in contact with the bone was only used HW 322, for more delicate work. Along the process, and always when required the bone surfaces were consolidated with Paraloid B-72 diluted in acetone at 5%, and any breaks or deep fissures were glued and reinforced with higher concentrations like 20% and 50%. The entire preparation process was extensively recorded with written documentation and accompanying photographs in Parque dos Dinossauros da Lourinhã (Portugal).

Measurements of the specimen ML2776 (Appendix 1) have been done following Puértolas et al. (2011).

The phylogenetic analysis was run using the TnT version 1.5 (Goloboff and Catalano, 2016), following the character matrix of Arribas et al (2019), which is based on Ristevski et al. (2018), as it is one of the most recent and complete phylogenetic matrices for Goniopholididae. A heuristic search algorithm (traditional search analysis) of maximum parsimony with tree bisection reconnection was done, with one random seed, 1000 replications, and saving 10 trees per replication.

Branch support was calculated using standard Bootstraps resampling with the following options: 1000 number of replicates, using the consensus tree, searching trees with the traditional search, and an output result as absolute frequencies. The Bremer supports were done using the 'Bremer.run'

script, saving up to 1000 suboptimal trees instead of 10 suboptimal trees as in Arribas et al. (2019).

For ancestral state analyses, the program MESQUITE (Maddison and Maddison, 2018) was used to reconstruct the ancestral state, using the method of maximum-likelihood-Mk1.

Institutional abbreviations. **AR**, Ariño collection, Museo Aragonés de Paleontología, Teruel, Spain; **IRSNB**, Institut Royal des Sciences Naturelles de Bruxelles, Belgium; **ML**, Museu da Lourinhã, Lourinhã, Portugal; **PDL**, Parque dos Dinossauros da Lourinhã, Lourinhã, Portugal; **SMM**, Science Museum of Minnesota, Saint Paul; USA.

SYSTEMATIC PALEONTOLOGY

Superorder CROCODYLOMORPHA Hay, 1930
(sensu Walker, 1970)

Clade CROCODYLIFORMES Hay, 1930
Suborder MESOEUCROCODYLIA Whetstone and Whybrow, 1983 (sensu Benton and Clark, 1988)
Infraorder NEOSUCHIA Gervais, 1871 (sensu Benton and Clark, 1988)

Family GONIOPHOLIDIDAE Cope, 1875
Genus *OPHIUSSASUCHUS* gen. nov.

zoobank.org/7828D79B-2773-4F0C-94E8-4F0CFB443597

Etymology. '*Ophiussa*' refers to the ancient name given by the Greeks to the area where is now Portugal; and '*suchus*' is from the Greek *souchos* that refers to crocodile-headed Egyptian god Sobek.

Diagnosis. As for the type species.

Type species. *Ophiussasuchus paimogonectes* gen. et sp. nov.

OPHIUSSASUCHUS PAIMOGONECTES sp. nov.
Figures 1-3

zoobank.org/F31747D6-B166-4DD0-90D8-6443FD97A073

Holotype. ML2776, an almost complete and well-preserved isolated skull, with some teeth still attached. The specimen is deposited at Lourinhã Museum (Museu da Lourinhã), Lourinhã, Portugal.

Etymology. '*paimogonectes*' refers to the one who swims in Paimogo, where the specimen was found (Paimogo beach, Lourinhã, Portugal).

Age and horizon. Praia Azul Member, Lourinhã Formation, Lusitanian Basin, west coast of Portugal. upper Kimmeridgian-lower Tithonian, Upper Jurassic.

Type locality. Praia de Paimogo (GPS coordinates: 39° 17' 10.4" N, 9° 20' 17.4" W), Lourinhã, Lisbon, Portugal.

Diagnosis. Medium-sized crocodylomorph about 2.5 m to 3 m long (estimated body length based on Young et al., 2011), with platyrostral, mesorostrine skull and a marked festooned contour which differs

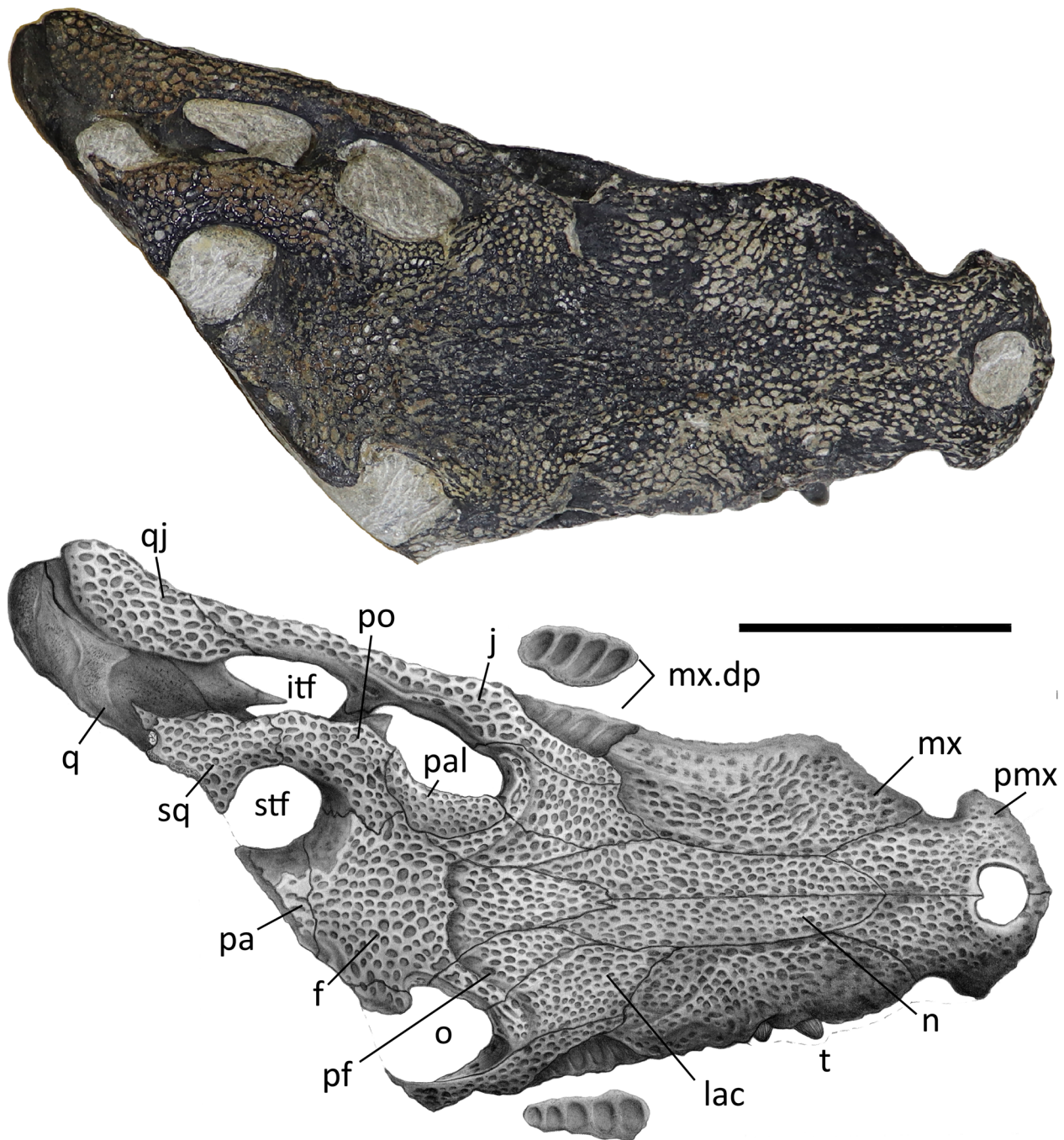


FIGURE 1. Skull of ML2776 *Ophiussasuchus paimogonectes* gen. et sp. nov., in dorsal view. Anatomical abbreviations: **f**, frontal; **itf**, infratemporal fenestra; **j**, jugal; **lac**, lacrimal; **mx**, maxilla; **mx.dp**, maxillary depressions; **n**, nasal; **o**, orbit; **pa**, parietal; **pal**, palpebral; **pf**, prefrontal; **pmx**, premaxilla; **po**, postorbital; **q**, quadrate; **qj**, quadratojugal; **sq**, squamosal; **stf**, supratemporal fenestra; **t**, tooth. Scale represents 10 cm. Image by C. Pineda.

from other goniopholidids since it possess a less pronounced axe-shaped premaxillae dorsal outline; smooth perinarial region with absence of crests around it; presence of different number of maxillary depressions between the left and right

regions (four and five, respectively); anteriorly well-marked V-shape border of the palatines in contact with the maxillae; nasals with straight, sub-parallel margins between the maxillae, with little to no lateral expansion at their posterior-most border; main

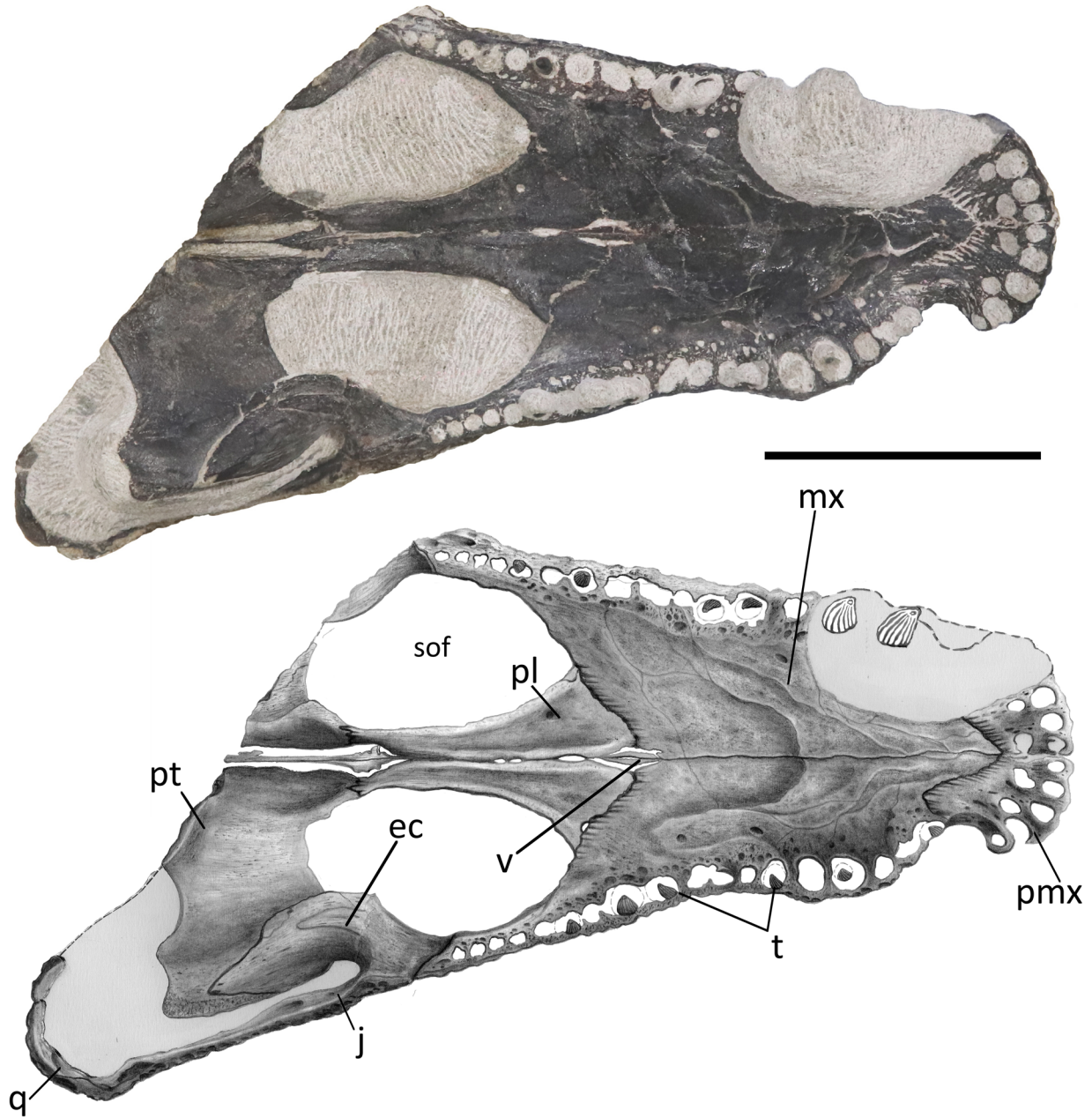


FIGURE 2. Skull of ML2776 *Ophiussasuchus paimogonectes* gen. et sp. nov., in ventral view. Anatomical abbreviations: **ec**, ectopterygoid; **j**, jugal; **mx**, maxilla; **pmx**, premaxilla; **pl**, palatine; **pt**, pterygoid; **q**, quadrate; **sof**, suborbital fenestra; **t**, tooth; **v**, vomer. Scale represents 10 cm. Image by C. Pineda.

body of the frontal with sub-squared shape in dorsal view, without lateral expansion; nasopharyngeal duct less ventrally exposed than in Jurassic taxa (e.g., *Calsoyasuchus* or *Eutreptauranosuchus*) but not as closed as in Cretaceous taxa (e.g., *Hulkepholis* or *Anteophthalmosuchus*); presence of two small, thin, anteroposteriorly elongated and crescent-shaped palatal fenestrae between the maxillae and the palatines.

DESCRIPTION

ML2776 is a partial mesorostrine skull of a goniopholidid (Figures 1-3), approximately 30 cm of total length (from the tip of the snout to the estimated position of the occipital condyle, because it is not preserved) and 38 cm from the tip of the snout to the posterior end of the quadrate condyle (all the measurements were updated to Morpho-

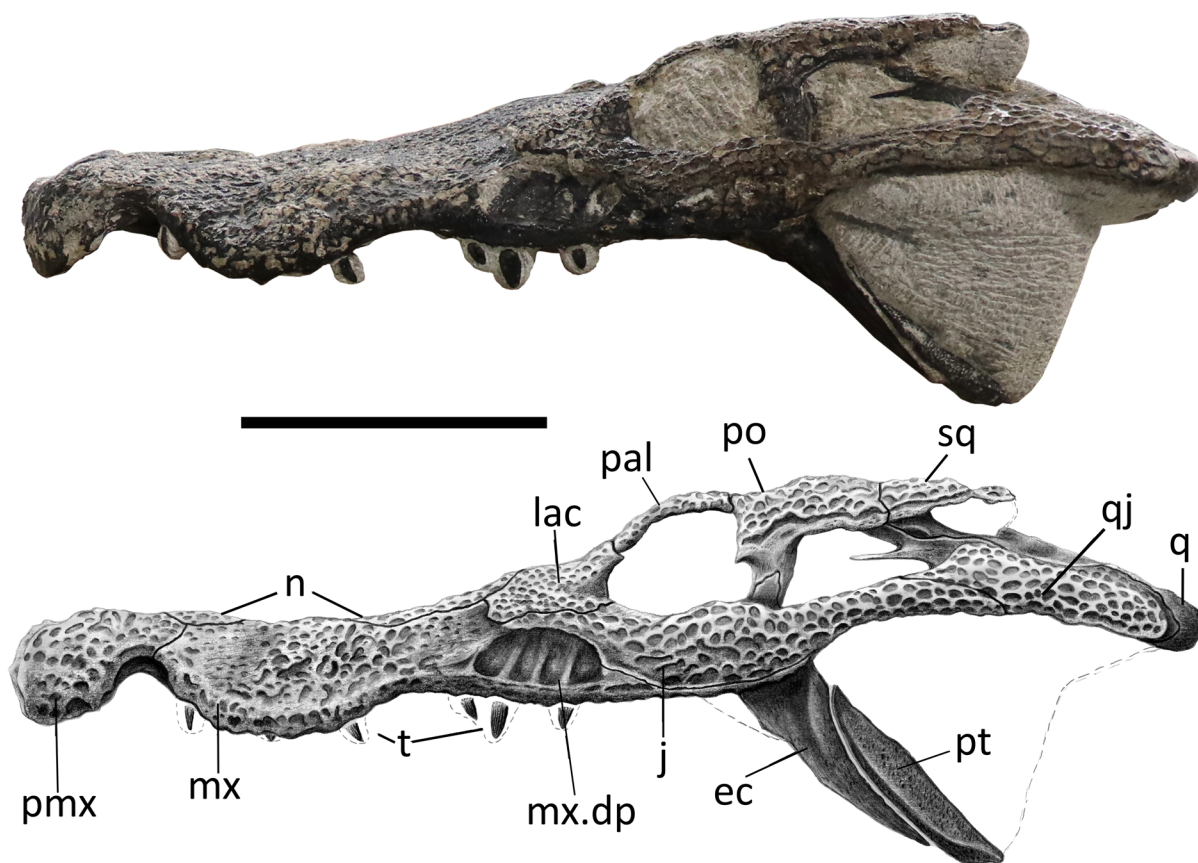


FIGURE 3. Skull of ML2776 *Ophiussasuchus paimogonectes* gen. et sp. nov., in lateral view. Anatomical abbreviations: **ec**, ectopterygoid; **j**, jugal; **mx**, maxilla; **mx.dp**, maxillary depressions; **n**, nasal; **pal**, palpebral; **pf**, prefrontal; **pmx**, premaxilla; **po**, postorbital; **pt**, pterygoid; **q**, quadrate; **qj**, quadratojugal; **sq**, squamosal; **t**, tooth. Scale represents 10 cm. Image by C. Pineda.

Bank, see Data Archiving Statement). The specimen is very well preserved, and nearly complete, just missing the posterior right end of the skull (from the posterior margin of the right orbit until the right quadrate, including the occipital region of the skull).

The skull is typically platyrostral, wider than high, and mesorostrine, in contrast with other longirostrine goniopholidids (e.g., *Hulkepholis willetti* Salisbury and Naish, 2011). As common in goniopholidids and eusuchian crocodylomorphs, the skull has no antorbital fenestra. In dorsal view (Figure 1), the skull gradually becomes wider posteriorly. This overall shape is shared with other *Goniopholis* species (Andrade et al., 2011), and closer looking to *G. baryglyphaeus* (Schwarz, 2002). All the dorsal surface of the skull is covered by the typical crocodylomorph ornamentation pattern based on sub-circular pits and grooves. Some areas lack ornamentation and are smoother, such as the max-

illary depressions and the quadrate. In contrast, the ventral surface of the skull lacks any ornamentation.

The premaxillae are completely preserved but missing the teeth. Each individual premaxilla is as dorsoventrally high as it is lateromedially wide. Together, both premaxillae are as lateromedially wide as they are anteroposteriorly long, but narrower laterally than the maxilla. As in most goniopholidids, the premaxilla has a deep lateral notch at the premaxilla-maxilla contact, giving it an axe-shaped dorsal outline, but not as pronounced as *Goniopholis kiplingi* Andrade, Edmonds, Benton, and Schouten, 2011. However, in *Ophiussasuchus paimogonectes* gen. et sp. nov., as well as in *Goniopholis simus* Owen 1878, the axe-shaped posterolateral border of the premaxilla, at the anterior margin of the notch, is more rounded in comparison to other goniopholidids where this margin is laterally projected and sharpened, as in *Goniop-*

holis kiplingi (Andrade et al., 2011) or *Amphicotylus stovalli* Mook, 1964 (Allen, 2012). Dorsally, the posterior process of the premaxilla wedges posteriorly between the maxilla and the nasal, until the level of the posterior margin of the third maxillary alveolus. The external naris appears in the anteriormost region of the premaxilla. It is sub-circular and slightly wider than long. The naris is facing dorsally although it has a slight anterodorsal component due to the anterior margin is slightly lower than the posterior margin, differing from the fully dorsally orientated naris of *G. kiplingi* (Andrade et al., 2011). This narial inclination is not as marked as in taxa considered to have anterodorsal naris orientation such as the basal goniopholidid *Calsoyasuchus* (Tykoski et al., 2002), the pholidosaurid *Sarcosuchus* (Serenó et al., 2001), or the thalattosuchian *Dakosaurus* (Pol and Gasparini, 2009). The external naris is displayed by a confluent opening of the nares, without an internarial bar. In anterior view, the anterior margin of the naris is slightly dorsally elevated in the sutural contact of both premaxillae. The posterior margin of the naris is completely formed by the premaxillae, without any participation of the nasals. There is a tiny anterior projection of the premaxilla into the posterior margin of the naris. The margins of the naris are smooth without the presence of any associated crest or grooves around it. This character contrasts with other goniopholidids such as *Amphicotylus* (Yoshida et al., 2021), *Hulkepholis willetti* (Salisbury and Naish, 2011), or the other species of *Goniopholis* where the perinarial crests are present (Andrade et al., 2011). The sagittal sutural contact of the premaxillae, posterior to the naris, is more than twice longer than the same suture anterior to the naris.

Ventrally (Figure 2), each premaxilla contains five circular alveoli ventrally oriented, with the last one anterior and parallel to the first maxillary tooth. The third and fourth premaxillary alveoli are the same size and are the largest, followed by size by the second alveolus, while the first and fifth alveoli are the smallest ones. In ventral view, a large pit can be found posteriorly between the first and second alveoli, and another pit posteriorly between the third and fourth alveoli. The premaxillae are ventrally fused, forming the anterior region of the secondary bony palate, only pierced by a very small, slit-like shape, incisive foramen (=naso-oral fenestra, Andrade et al., 2011) in the medial region, between the two large pits. This incisive foramen can also be seen in *Amphicotylus stovalli* (Allen, 2012, figure 3), *Amphicotylus lucasii* Cope, 1878

(Erickson, 2016, figure 1b), and *Hulkepholis plotos* Buscalioni, Alcalá, Espílez, and Mampel, 2013 (Arribas et al., 2019, figure 2c). Smaller neurovascular foramina medial to the alveolar region can be observed. The ventral posterior process of the premaxilla expands into the maxilla, reaching the level between the second and third maxillary alveoli, with an acute sagittal anterior process of the maxillae making a V-shape sutural contact, similar to other taxa such as *G. simus* (Karl et al. 2006) and *Am. Lucasii* (Erickson, 2016), and in contrast to *Am. Stovalli* (Allen, 2012) and *H. plotos* (Buscalioni et al., 2013) where it is more round-shape. This contact does not reach the incisive foramen, as in *Am. Lucasii* (Erickson, 2016), but in contrast to *Am. Stovalli* (Allen, 2012). There are small scars or striations along the premaxilla following the premaxilla-maxilla sutural contact. Similar striations can be observed in the illustration of *Am. Lucasii* in Erickson (2016).

Both maxillae are well preserved, including several teeth. Only the anterior lateral margin of the right maxilla, from the level of the first until the sixth maxillary teeth, is slightly eroded. In dorsal view, the maxilla shows a lateral festooned outline, a common feature in most goniopholidids, but very subtle in taxa such as *Eutretauranosuchus* (Smith et al., 2010; Pritchard et al., 2013), and almost not present in *Calsoyasuchus* (Tykoski et al., 2002; Allen, 2012; Arribas et al., 2019) and *Sunosuchus* (Wu et al., 1996). In dorsal, ventral, and lateral views, at the premaxillary-maxillary suture, the maxilla shows its greatest concavity coinciding with the notch for the reception of the largest dentary tooth. Although the notch is well marked, it just encases the lingual, and partially the anterior and posterior surfaces of the crown of the dentary tooth, while the labial surface of the tooth would remain completely laterally open. In dorsal and ventral views, while the anterior premaxillary margin of the notch expands more abruptly, the posterior maxillary margin of the notch progressively expands laterally until the maxilla reaches its maximum width at the fifth alveolus, where it gets a convex contour. Posteriorly, from this point of maximum convexity, the maxilla narrows again to get another subtle concave profile, with its maximum concavity at the level of seventh-eighth teeth. Posteriorly to this area, the margins of the maxilla in dorsal and ventral profiles are followed by a second, but less marked, lateral convexity, coincidental with the lateral maxillary depression, from where it approximately keeps the same width until its posterior end. In lateral view (Figure 3), the

same festooned profile that was in dorsal view can be observed. The maximum ventral projection of the maxilla coincides with the maximum lateral projection, and it reaches the same ventral height as the premaxilla alveolar margin. However, the second posterior convexity is less marked, so the ventral alveolar margin remains more dorsally placed. The anteromedial region of the maxilla is slightly expanded dorsally giving a swollen overall shape. This relief is located at the same level as the largest maxillary tooth and at the greatest lateral and ventral expansion of the maxilla, which is probably caused by the placement of the root of this tooth. This swollen region of the maxilla projects over the nasal region at the same point laterally, hiding the anterior region of the nasal in lateral view. In lateral view, a series of neurovascular foramina appear along the limit of the dorsolateral margin of the maxilla, without reaching the alveolar region, and get more dorsally posteriorly in the maxilla.

There are well-marked maxillary depressions at the posterolateral-most region of the maxilla (Figures 2–3), a feature shared with some pholidosaurids and most goniopholidids (e.g., Martin and Buffetaut, 2012; Martin et al., 2016; Yoshida et al., 2021). *Nannosuchus*, *Vectisuchus*, and the putative goniopholidid *Denazinosuchus*, do not show any maxillary depressions. However, it is unclear if the absence of depressions in *Nannosuchus* may be related to its putative juvenile ontogenetic stage (Andrade et al., 2011). These maxillary depressions start below the anterior margin of the lacrimal, at the same level as the tenth and eleventh maxillary alveoli, posteriorly reaching the region between the thirteenth and fourteenth maxillary alveoli. Most of the maxillary depression is slightly overlapped by the posterolateral region of the lacrimal and anterolateral margin of the jugal. There are four maxillary chambers in the left depression and five in the right one, showing a similar condition to *Am. lucasii* (specimen SMM P 2003.20.1), a taxon that also displays four chambers (Erickson, 2016, figure 2A). However, in *Am. lucasii*, the depressions occupy a wider region of the maxilla than in ML2776. Nevertheless, the presence of four chambers on the left side in ML2776 could be due to erosion or another factor, and the actual number could be five, as appears to be on the right side. If this was the case, this feature would be shared with the recently described North American Jurassic taxon *Amphicotylus milesi* Yoshida, Hori, Kobayashi, Ryan, Takakuwa, and Hasegawa, 2021, which is clearly five-chambered. In contrast, other goniopholidids display a smaller number of

chambers: having two in taxa such as *H. plotos* (Buscalioni et al., 2013) or *H. rori* (Arribas et al., 2019); or three as in *G. kiplingi*, *G. simus* (Andrade et al., 2011), and the specimen IRSNB R47 of *Anteophthalmosuchus epikrator* Ristevski, Young, Andrade, and Hastings, 2018 (= *Anteophthalmosuchus hooleyi* in Martin et al., 2016). The number of chambers in *G. baryglyphaeus* cannot be determined with certainty since its internal structure is partially eroded (Schwarz, 2002). However, given its subcircular shape, its short anteroposterior extension, and the fact that some of the internal ridges are partially preserved in *G. baryglyphaeus*, a maximum of three chambers within the fossa can be inferred. Regarding the chambers, some authors point out that the depth and subdivision of the maxillary depression is a variable character that increases with the ontogeny (Mook, 1921; Smith et al., 2010). However, some taxa represented by big specimens, larger than or like ML2776 (e.g., *G. kiplingi*, *G. simus*, or *An. hooleyi* IRSNB R47), have fewer chambers than ML2776. Therefore, although there could be some intraspecific variability related to ontogeny, the number of chambers could be a diagnostic character to compare different taxa with similar ontogenetic development. Although the individual chambers are not ornamented, presenting a smooth surface, the two posteriormost chambers have remains of the neurovascular opening in a mid-dorsal position, as other goniopholidids (Andrade et al., 2011). The chambers are more elongated dorsoventrally than anteroposteriorly and are separated by slightly posteriorly sloping dorsoventral ridges.

Ventrally, the maxillary palatal shelf is flat and smooth, with a line of foramina pattern medially to the alveoli. No pits or diastemas are observed between the dental alveoli, so an overbite occlusal pattern can be inferred. The maxilla holds a total of 18 alveoli, a feature that changes through species (e.g., *Am. lucasii* has 22 alveoli; Erickson, 2016), some of them still with the crown tooth preserved (six in the right maxilla and five in the left one). There are some lingual occlusion pits visible in the left maxilla, one posteromedial to the second alveolus, and another between the eighth and ninth alveoli. The teeth are vertically oriented and lingually curved, with pointed caniniform shape, with smooth carinae (not serrated) and circular cross-section. As in most goniopholidids, the fourth and fifth maxillary alveoli are almost the same size and the largest teeth, more than the largest premaxillary tooth (Allen, 2012; Erickson, 2016; Arribas et al., 2019). The enamel of the anterior maxillary

teeth is smooth, while the posterior maxillary teeth are ornamented by fine basi-apical anastomosed ridges close to each other. The tooth row of the maxilla starts after the premaxilla-maxilla notch and extends until the mid-region of the lateral margin of the suborbital fenestra, with the enlarged anterior and posterior teeth coincidental to the lateral and ventral convexity. In ventral view, the posteromedial region of the maxillae contacts with an anterior projection of the palatines, making an anteriorly V-shape border, in contrast to taxa such as *G. simus* (e.g., Salisbury et al., 1999; Karl et al., 2006) or *Am. stovalli* (Allen, 2012), *Am. milesi* (Yoshida et al., 2021), *An. hooleyi* (Salisbury and Naish, 2011; Ristevski et al., 2018), *An. epikrator* IRSNB R47 (= *An. hooleyi* in Martin et al., 2016) or *Eutreptauranosuchus delfsi* Pritchard, Turner, Allen, and Norell, 2013, where the contact between maxilla and palatine is blunter and transversal to the sagittal plane. The anterior margin of the palatines is more similar to that is present in *H. willetti* (Salisbury and Naish, 2011) and *C. valliceps* (Tykoski et al., 2002), although ML2776 presents an intermediate morphology with a less rounded tip than in *H. willetti* but not as acute as in *C. valliceps*. The posteromedial border of the maxilla makes part of the anterolateral margin of the suborbital fenestrae, displaying a rounded concave shape. Laterally to the intersection of the maxilla-palatine suture with the sagittal plane, between the palatines and the maxillae, two small anteroposteriorly elongated and crescent-shaped palatal fenestrae are observed (Figure 2). These two openings represent a palatogenesis where the palate is not completely fused in this region. Between these two fenestrae, two bony thin sheets that correspond to the vomers are exposed.

Both nasals are complete and well-preserved. The nasals display a long and slender shape, contacting the posterior region of the premaxilla, but not reaching the external naris. In dorsal view, the nasals have a sub-rectangular general shape, with straight and sub-parallel lateral margins contacting extensively with the medial margin of the maxilla. The overall sub-parallel lateral margins of the nasals are common in most goniopholidids (Andrade et al., 2011; Buscalioni et al., 2013; Arribas et al., 2019). However, in the posterior region where the nasal meets the lacrimal, the nasal still displays lateral sub-parallel margins with little lateral expansion. This display contrasts with most goniopholidids such as *Anteophthalmosuchus* (Salisbury and Naish, 2011; Martin et al., 2016; Ristevski et al., 2018), *Goniopholis* (Salisbury et

al., 1999; Andrade et al., 2011), *Hulkepholis* (Salisbury and Naish, 2011), or the undetermined goniopholidid AR-1-3422 from Ariño (Spain) (Buscalioni et al., 2013), which show a concave lateral expansion in the posterior region of the nasal. The nasals have a pointed anterior convergence, wedging between the premaxillae, while diverging in the posterior end, wedging between the frontal, lacrimal, and prefrontal. The posterior end of the nasal, in dorsal view, does not reach the anterior orbital margin level, such as in AR-1-3422 specimen (Buscalioni et al., 2013), *G. kiplingi* (Andrade et al., 2011), and *Hulkepholis willetti* (Andrade et al., 2011; Salisbury and Naish, 2011). In other goniopholidids, such as *G. simus*, (Andrade and Hornung, 2011) or *Am. stovalli* (Allen, 2012), the posterior end of the nasal surpasses the level of the anterior orbital edge. In ML2776 and most goniopholidids, the prefrontal-nasal medial and lateral contacts form a continuous straight line, however, in *H. willetti* (Andrade and Hornung, 2011; Salisbury and Naish, 2011) and, to a lesser degree, in *G. baryglyphaeus* (Schwarz, 2002), the prefrontal wedges a small anterior process into the lateral margin of the nasal. In lateral view, the anterior nasal region is hidden by a dorsal swelling of the maxilla, a common feature in most goniopholidids. This feature is difficult to contrast with other specimens, as the representations are mostly from dorsal view, but it is found in *Am. lucasii* (Erickson, 2016, figure 2).

Both lacrimal are complete and well preserved, only the right lacrimal is slightly eroded, so the suture with the anteromedial region of the jugal is faint and difficult to distinguish. The lacrimal is a little longer than wide, anteriorly wedging between the posterior regions of the nasal and the maxilla, reaching between the tenth and eleventh maxillary teeth position and separating the maxilla from the prefrontal. The posterior border of the lacrimal makes a shallow fossa over the anterior-most region of the orbit, without participating in the ventral border of the orbit. In dorsal view, the anterior border of the orbit is closed into a narrow enclosure, produced by the elevated posterior edge of the lacrimal.

The left jugal is well preserved and complete, while only the anterior-most portion of the right jugal is poorly preserved. It has a sub-elliptical blade shape, flattened lateromedially. The jugal is broad in its anterior region and gets narrower posteriorly. Dorsally, the jugal is a long and straight bone, while laterally has a slight sigmoidal shape. The jugal wedges anteriorly between the lacrimal and the maxilla until the level of the anterior sec-

ond chamber of the maxillary fossa, while the posterior contact of the jugal with the quadratojugal is subtle, almost transversal to the sagittal plane. In lateral view, the jugal contacts with the posterior region of the maxilla by overlapping it. The anterolateral region of the jugal is dorsoventrally flattened, dorsally overlapping the three last chambers of the maxillary depression, reaching anteriorly the position between the eleventh and twelfth alveoli, with a similar contribution to the rostrum region as other goniopholidids, such as *Amphicotylus* (Erickson, 2016), *Goniopholis* (Andrade et al., 2011), *Hulkepholis* (Salisbury and Naish, 2011), or *Anteophthalmosuchus* (Martin et al., 2016). The lateroventral border of the orbit is made completely by the anteromedial margin of the jugal while the posteromedial margin of the jugal participates in the lateral border of the infratemporal fenestra. In lateral view, the jugal is ventrally convex and dorsally straight below the orbit, while the jugal bar is concave ventrally and straighter dorsally. At the level where the ventral region of the postorbital bar contacts with the jugal, the dorsal margin of the jugal is slightly raised forming a crest, dorsally wedging into the bar. The ascending ramus of the jugal in the postorbital bar is not ornamented, and the postorbital bar is subcircular in cross-section. The lower temporal bar is flattened as it is dorsoventrally higher than mediolaterally wide.

The prefrontals are slender and almost twice as long than wide. The anteromedial border of the prefrontal contacts with the posterolateral region of the nasal, and the medial border contacts with the lateral margin of the anterior process of the frontal. The anterior-most tip wedges between the nasal and the lacrimal. The posterolateral border of the prefrontal is flat, following the lacrimal, while the dorsal projection of the palpebral forms a crest on the anterolateral region of the orbit, without overhanging it. The prefrontal contribution to the medial border of the left orbit is obscured by the presence of a large palpebral bone. However, in the right orbit, where the palpebral bone is not preserved, the prefrontal participation in the anteromedial margin of the orbit is visible. The prefrontal shape variability is wide among goniopholidids, which can be seen in the comparison made by Arribas et al. (2019). In dorsal view, *Anteophthalmosuchus* displays a thick posteriorly expanded prefrontal, while in *Goniopholis* and *Hulkepholis*, the posterior region of the prefrontal is slenderer and more curved to the orbit, more like what *Ophiussasuchus paimogonectes* gen. et sp. nov. displays.

Just the left palpebral is complete and well preserved. It is sub-triangular, robust, and large, contributing to most of the medial margin of the orbit. Although the right palpebral is not preserved, there is a groove or scar, over the posterolateral surface of the prefrontal and part of the frontal, for the palpebral attachment and showing a strong and extensive attachment with the skull roof. The orbital margin of the palpebral projects dorsally, with the lacrimal, forming a crest on the anteromedial region of the orbit, but without overhanging the orbit. Without the palpebral, the orbit faces dorso-laterally rather than laterally.

The frontal is almost complete, completely fused, missing only its posteriormost right portion. The frontal is wide and flat, without the presence of a sagittal crest or a sagittal suture, contributing to most of the preserved portion of the skull roof. The main body of the frontal is ventrally depressed relative to the swollen postorbital and squamosal, therefore the skull roof is not flat but concave. The main body is flat, with a rectangular shape, projected anteriorly, and wedging into the nasals with a truncated anterior tip. This anterior process surpasses the prefrontals and reaches the eleventh and twelfth maxillary tooth position. The anterior process lays more ventral than the main body of the frontal, with a transverse interorbital crest that creates a step between them. The lateral regions of the main body of the frontal (between the orbits and the supratemporal fenestrae) are less laterally expanded than in most goniopholidids such as *G. kiplingi* (Andrade et al., 2011), *Nannosuchus* (Andrade and Hornung, 2011), *Hulkepholis* (Arribas et al., 2019), or *Anteophthalmosuchus* (Martin et al., 2016; Ristevski et al., 2018), in which the frontal shows a T-shape in dorsal view. In fact, the lateral margins are more like the proportions observed in *G. baryglyphaeus* (Schwarz, 2002), *G. simus* (Karl et al., 2006; Andrade and Hornung, 2011), or *Eutretauranosuchus* (Pritchard et al., 2013). The frontal slightly contributes to the medial margins of the orbit, as in other goniopholidids (Andrade et al., 2011; Andrade and Hornung, 2011), which can be seen in the right orbit, where the palpebral is missing, while in the left orbit the palpebral covers the frontal contribution to the orbit. The frontal contribution to the supratemporal fenestra is reduced to a small portion in its anteromedial border where a shallow and smooth fossa is developed. This contribution of the frontal to the supratemporal fenestra contrasts with most goniopholidids (Andrade et al., 2011; Andrade and Hornung, 2011; Allen, 2012; Ristevski et al., 2018)

where the frontal contributes to almost the entire anteromedial margin of the supratemporal fenestra. In ML2776, it is more like the condition present in *Calsoyasuchus* (Tykoski et al., 2002) or *Hulkepholis* (Salisbury and Naish, 2011; Buscalioni et al., 2013). In dorsal view, the supratemporal fossa displays a sub-square shape, with rounded corners, while the supratemporal fenestra has a tear-drop shape, with the anterolateral border narrower than the posteromedial one. Both fossa and fenestra, however, have no significant difference in size, with a similar size to the orbit.

The left postorbital is complete and well preserved but partly covered by the palpebral. Just the anterior-most portion of the right postorbital is preserved. Dorsally, the postorbital has a crescent shape surrounding the anterolateral corner of the supratemporal fenestra. It represents about half of the upper temporal bar. In dorsal view, the temporal bars are sub-parallel, with a sinusoidal shape, giving a rectangular shape to the skull roof. The postorbital contributes anterolaterally with the posterodorsal border of the orbit. There is a short anterior projection of the anterolateral region of the postorbital over the orbit, almost at the same level as the descending process of the postorbital bar. This condition can be seen also in *G. simus* (Andrade and Hornung, 2011) or *Am. lucasii* (Erickson, 2016). The postorbital contributes laterally to the dorsal border of the infratemporal fenestra. There is a descending process, with a clear separation from the main body of the postorbital, that forms the dorsal portion of the postorbital bar. The dorsal region of the postorbital bar has two anterolateral projections (or spines) and vascularity pitting in the lateral region. The bar is robust, cylindrical, and slightly inclined in anterior view and vertical in lateral view. The bar also contributes anteriorly to the posterodorsal border of the orbit, and posteriorly to the anterodorsal border of the infratemporal fenestra.

In lateral view, the infratemporal fenestra, only preserved in the left region of the skull, is a big fenestra a bit smaller than the orbit. It is longer than high, with a sub-polygonal shape as in *G. kiplingi* (Andrade et al., 2011; Allen, 2012), *Am. lucasii* (Erickson, 2016), and *An. hooleyi* (Ristevski et al., 2018). The infratemporal fenestra is visible in dorsal view, as it faces laterodorsally, therefore it is not covered by the upper temporal bar.

The left squamosal is incomplete but well preserved, missing the posteromedial region. The squamosal has a flat dorsal surface, widening posteriorly, and inclined slightly medially. In lateral

view, the preserved anterior squamosal region shows a faintly posteroventral concavity, giving the sinusoidal appearance seen in other crocodylomorphs (Arribas et al. 2019). The anteromedial border of the squamosal contributes to the posterolateral border of the supratemporal fenestra. Posteriorly, the broken region of the squamosal displays a dorsoventrally compressed sub-elliptical cross-section. In the posterolateral region of the squamosal, it develops a thin lateral projection coincidental to the otic area. The posterior squamosal lobes are not preserved.

Only a small portion of the anteriormost region of the parietal is preserved due to erosion. The preserved parietal is fused in a single flat bone. Its lateral border contributes to the medial region of the supratemporal fenestra. The suture with the frontal is also poorly preserved, however, it is almost straight and transversal to the sagittal plane. The frontoparietal suture is situated posterior to the orbits and to the postorbital bar, and in a very anterior position in comparison to *Goniopholis* (Andrade et al., 2011; Erickson, 2016), *Hulkepholis* (Andrade and Hornung, 2011; Arribas et al., 2019) and *Calsoyasuchus* (Tykoski et al., 2002), where the suture is situated at the half of the bar between the supratemporal fenestrae. In posterior view, the parietal displays a concavity, facing ventrally, that corresponds to the portion of the braincase related to the parietal region.

The left quadratojugal is complete and well preserved, displaying the pitting ornamentation in most of its laterodorsal region. The ventral region, and the area in contact with the quadrate, are smooth and lack any ornamentation. Dorsally, a well-marked step delimits the ornamented region from the smooth area, as seen in most goniopholidids (Andrade et al., 2011; Erickson, 2016; Martin et al., 2016). The quadratojugal has a convex dorsal surface, while the ventral surface is more concave. The sinusoidal suture with the jugal lies very close to the posteroventral border of the infratemporal fenestra, with the anterior region of the quadratojugal contributing to the ventral and posterior border of this fenestra. There is a dorsomedial projection contacting locally with the ventral posterior region of the postorbital, making part of the posterior and posterodorsal border of the infratemporal fenestra. From the posterior border of the infratemporal fenestra, there is a long projection of the quadratojugal in its upper distal region, the quadratojugal spine (or spina quadratojugal, as in Arribas et al., 2019). It projects anteriorly and parallel to the ventral border of the fenestra, and

almost reaching half the length of the infratemporal fenestra.

The left quadrate is almost complete and well preserved, missing most of the medial region. The quadrate displays an almost horizontal shaft, with the posteriormost region slightly ventrally oriented. The lateral condyle is posteriorly projected, exposing the posteriormost smooth surface of the quadrate. In dorsal view, there is a small concavity in the contact with the lateral condyle of the quadrate and the quadratojugal. The small portion preserved from the medial condyle shows that the posteroventral region of the quadrate, the articulation surface with the mandible, displays a small concave surface between both condyles. A siphonal foramen is present on the dorsomedial surface of the quadrate, anterior to the otic opening.

The palatines are complete and well preserved, displaying a smooth, slim, and almost horizontal surface. In ventral view, they are pierced by the two thin and slender maxillo-palatine fenestrae in their anteriormost region (anterior palatal fenestrae already described in the maxilla section). The anterior process of the palatines surpasses the anterior margin of the suborbital fenestrae, it is short and wedges into the posteromedial region of the maxillae with a V-shaped contour. The maxilla has a small process, a subtle medial projection on the posterolateral border of the anterior process of the palatine. Ventrally, the palatines are partly in contact medially until the height of the last maxillary tooth. Posterior to the two crescent-shaped fenestrae, a single small teardrop-shaped opening is situated on the sagittal suture of the palatines. The ventral and lateral borders of the palatines enclose a narrow nasopharyngeal duct that is not completely fused in some areas of the sagittal region. This duct opens posteriorly into the internal choana at the height of the palatine-ptyergoid suture. The medial posterior palatines form the anteriormost lateral margin of the internal choana. The straight lateral borders of the palatines form the anteriormost and medial rounded borders of the large suborbital fenestra, which are more than twice the size of the orbits.

The presence of two isolated palatal fenestrae between the maxillae and the palatines has also been reported in some basal goniopholidids from the Late Jurassic of Asia such as *Sunosuchus junggarensis* Wu, Brinkman, and Russell, 1996 and *Sunosuchus miaoi* Young, 1948 (Buffetaut, 1986). However, these fenestrae are much larger and wider in the two Asian taxa than in ML2776. Similar palatal openings have also been observed

in the basal goniopholidids from the Jurassic of North America *Amphicotylus* (Allen, 2012; Erickson, 2016; Yoshida et al., 2021), *Eutreptauranosuchus* (Smith et al., 2010; Pritchard et al., 2013), and *Calsoyasuchus* (Tykoski et al., 2002). However, the palate in these American taxa is more open than in ML2776, and therefore the nasopharyngeal duct is more exposed in ventral view. In contrast, the more deeply nested Cretaceous European goniopholidids, such as *Goniopholis* (Salisbury et al., 1999; Karl et al., 2006; Andrade et al., 2011), *Hulkepholis* (Salisbury and Naish, 2011), and *Anteophthalmosuchus* (Salisbury and Naish, 2011; Martin et al., 2016), lack the anterior palatal fenestrae, have the nasopharyngeal duct totally closed, and the secondary choana only opens posteriorly between the contact of the palatines and the pterygoid. Therefore, ML2776 seems to present an intermediate palatogenesis development between the Jurassic North American and Asian goniopholidids and the Cretaceous European taxa.

The left pterygoid is completely preserved, while only the anterior-most region of the right one is preserved. The pterygoid displays the typical smooth, flat well-developed wing, expanded posteroventrally, reaching the height of the squamosal lobe. In ventral view, the anterior region of the pterygoid makes up most of the posterior border of the suborbital fenestra. The medial border of the pterygoid forms most part of the lateral choanal groove. The choanal grooves are smoothly exposed at the end of the nasopharyngeal duct, between the palatine-ptyergoid suture and the choanal septum. These grooves form a large diamond-shaped external choana, whose boundaries are not neat, as they open progressively forming a fossa on the ventral surface of the pterygoids. Except for its most anterior margin formed by the palatines, the rest of the choana is formed by the pterygoids. Even though the posterior border of the choana is not fully preserved, it can be deduced that it is not close to the posterior region of the pterygoids. The choanal septum (=interchoanal septum in Arribas et al., 2019) is a long and slender vertical wall of bone in the sagittal plane that divides the internal choana and the nasopharyngeal duct into two separate grooves and ducts. The anterior region of the choanal septum is wider and slightly expanded laterally at the anterior margin of the external choana, and a sagittal suture dividing the septum seems to be observed.

The left ectopterygoid is complete and well preserved, whereas only the anteromedial region of the right ectopterygoid is preserved. The

ectopterygoid is stout and smooth, and it is connected to the anterior pterygoid by a ventral wing-like projection (Figure 2). It contacts the maxilla anteriorly, the jugal laterally, and the pterygoid posteriorly, and makes part of the posterolateral border of the suborbital fenestra. In ventral view, the margin of the suborbital fenestra is bowed medially, creating a concave outline in this region of the fenestra. Its anterolateral end, on the posterior ramus of the maxilla, is short, reaching the level of the last maxillary alveolus but without touching or abutting the tooth row, as in other goniopholidids (Maisch et al., 2003; Salisbury and Naish, 2011; Martin et al., 2016). Its posterior flat acute tip does not reach the posterior margin of the pterygoid wing. Its dorsomedial involvement in the postorbital bar is short and limited only to the region near the base of the bar.

PHYLOGENETIC ANALYSIS

The analysis was performed following the character coding and matrix of Arribas et al. (2019). As in Arribas et al. (2019), most of the characters were equally weighted, except for the 26 characters that were ordered in Ristevski's dataset (Ristevski et al., 2018). A maximum parsimony heuristic search algorithm with tree bisection reconnection was performed, saving 10 trees per replication, with 1000 replications done. A standard Bootstraps resampling and Bremer supports (up to

1000 suboptimal trees) were also calculated and represented in the consensus tree (Figure 4).

The cladistic analysis recovered a total of two most parsimonious trees, with a tree length of 2378 steps. The analysis got a consistency index (CI) of 0.280, a retention index (RI) of 0.760 and a rescaled consistency index (RC) of 0.2128. In both trees, the specimen ML2776 is recovered as a sister taxon of the clade *Hulkepholis* + *Anteophthalmosuchus*. In the strict consensus tree (Figure 4), the specimen ML2776 is recovered with the unique combination of 15 unambiguous synapomorphies: absence of perinarial crest (character 29 = 0) and postnarial fossa (character 41 = 0); a straight morphology of the lateral border of the nasals, in dorsal view, posterior to the external nares (character 76 = 1); the suture between the frontal and the parietal is posterior to the postorbital bar, however, it does not reach the mid skull roof (character 122 = 1); the lateral temporal fenestra displaying an elliptic shape (character 164 = 0); maxilla and jugal ventral border not levelled, the maxilla fitting in a lower level with the jugal (character 184 = 1); the maxilla-palatine fenestrae present and anteroposteriorly elongated (character 205 = 2); absence of palatal shelves of the palatine (character 213 = 0); vomer exposed on the palate, between the maxilla and the palatine (character 221 = 2); palatines with a wide shape posteriorly while tapering anteriorly, wedging between the palatine rami of the maxilla (character 224 = 1); anterior border of the choana close to the posterior end of the nasopharyngeal

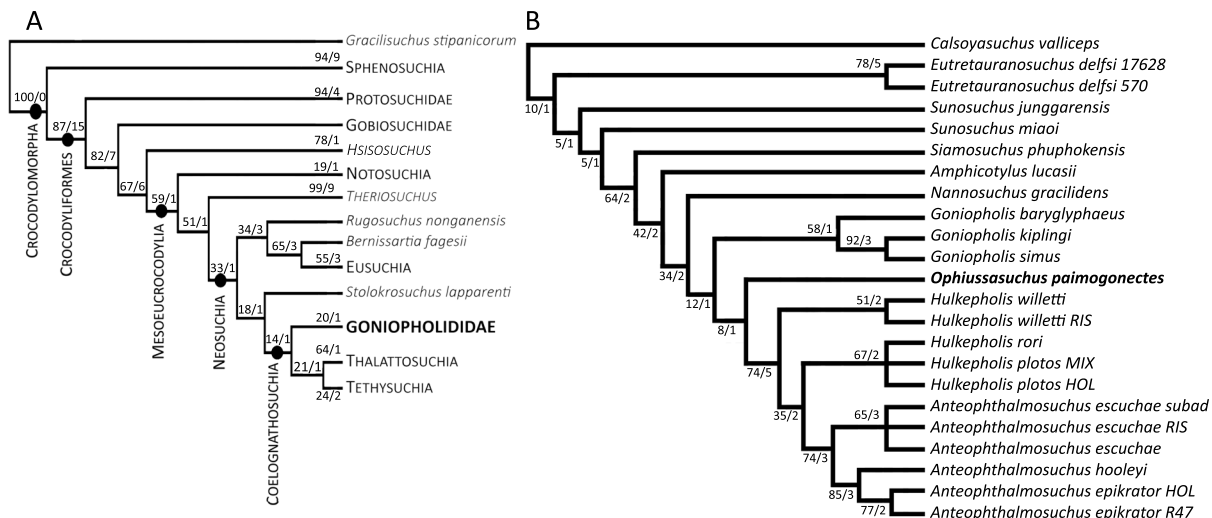


FIGURE 4. Phylogenetic analyses, with the Bootstraps and Bremer supports in each node. A. Simplified strict consensus cladogram, result from the two most parsimonious trees of 2381 steps following Arribas et al. (2019); B. Strict consensus of the Goniopholididae clade. *Ophiussasuchus paimogonectes* gen. et sp. nov. is recovered as the sister taxa of the clade *Hulkepholis* + *Anteophthalmosuchus*.

duct (character 235 = 2); slender teeth apically sharpened in the anterior to mid dentition (character .373 = 0); mid (character 383 = 1) and posterior (character 384 = 1) maxillary dentition overbites the mandibular ones; and anterior position of the last premaxillary tooth in relation to the first maxillary tooth, slightly altered relative to it (character 391 = 1).

DISCUSSION

Authors had an issue with the character coding criteria in Arribas et al. (2019) regarding the goniopholidids.

The species *Eutretraunosuchus delfsi*, specimen AMNH FARB 570 (Pritchard et al., 2013) codified as *Eutretraunosuchus delfsi* 570 in the matrix of Arribas et al. (2019) had a series of characters that were coded as state 2, while the only available states were 0 or 1. In Appendix 2, we describe how we recoded those characters, based on the published material in Pritchard et al. (2013).

In the character 110 (supratemporal fossae, orientation of the main axis at late ontogeny), none of the goniopholidids (with the exception of *Eutretraunosuchus delfsi* 110 = 1 and *Sunosuchus junggarensis* Wu, Brinkman, and Russell, 1996 110 = 1) are coded, while there are several well-preserved specimens, such as the skull of *Amphicotylus lucasii* (Erickson, 2016), *Goniopholis kiplingi* (Andrade et al., 2011), *Anteophthalmosuchus epikrator* (Martin et al., 2016), or *Hulkepholis willeti* (Salisbury and Naish, 2011) where the orientation of the main axis of the supratemporal fossae are also parallel, therefore in the present manuscript these taxa have been accordingly coded as 110 = 1.

The character 141 (frontal, participation in the primary medial border of orbit, at dorsal skull roof) Arribas et al (2019) created a new character state 2 in which the *Goniopholis* species show no participation in the medial primary border of the orbit. However, as Andrade and Hornung (2011) explain, in these taxa, and in others such as *Nannosuchus*, it seems that the frontal does not contact the orbit, but this is an artifact due to the presence of the palpebral bone. If we remove the palpebral, the frontal participates in the primary dorsomedial margin of the orbit, although this participation is small. This condition can be seen in *Ophiussasuchus paimogonectes* gen. et sp. nov. (Figure 1), in which the left side has the palpebral preserved, covering the distal frontal and hiding its participation in the medial edge of the orbit. However, on the right side, the palpebral is missing and the frontal partic-

ipation to the medial orbit can be seen. Even though its participation is minimal, the frontal participates in the medial border of the orbit. Consequently, character status 2 has been removed and the *Goniopholis* (*G. baryglyphaeus*, *G. kiplingi*, and *G. simus*) species have been recoded as 141 = 1.

In character 375 (mid to posterior dentition, presence and morphology of ridged ornamentation on the enamel surface of teeth) we coded the character as having both states “1” (present, composed of basi-apical well-defined ridges, conspicuous and set apart to each other) and “2” (same as state 1 but rarely anastomosed). The reason for this coding is that ML2776 presents the basi-apical well-defined ridges, but some of the teeth seem to present some type of very subtle anastomosis, but generally, it is absent.

The relationships between *Ophiussasuchus paimogonectes* gen. et sp. nov. and the other goniopholidids are well resolved, although not very well supported with low Bootstrap and Bremer supports, and ML2776 is recovered as the sister-taxon of the clade *Hulkepholis* + *Anteophthalmosuchus*. However, while *Hulkepholis* and *Anteophthalmosuchus* are Cretaceous taxa (Valanginian–Albian) (Buscalioni et al., 2013), *Ophiussasuchus paimogonectes* gen. et sp. nov. is a Late Jurassic species (Kimmeridgian–Tithonian), closer in time with the genus *Goniopholis*, which has a geobiochronological interval from the Late Jurassic to the Early Cretaceous (Kimmeridgian–Berriasian), and even closer to the Late Jurassic species *G. baryglyphaeus* locality (Schwarz, 2002). Moreover, some of the synapomorphies of ML2776 are shared with older species from North American species, such as *Calsoyasuchus* (Pliensbachian, Early Jurassic) or *Amphicotylus* (Kimmeridgian–Tithonian, Late Jurassic), rather than to the later taxa (*Goniopholis*, *Hulkepholis*, or *Anteophthalmosuchus*) while displaying a closer phylogenetic relationship with the European Cretaceous taxa.

The skull length range of the goniopholidids can be brevirostrine (*Nannosuchus*), mesorostrine (*Goniopholis* or *Ophiussasuchus paimogonectes* gen. et sp. nov.), or longirostrine (*Hulkepholis* and *Anteophthalmosuchus*). The rostrum region of ML2776 is similar in shape to *Goniopholis* and *Amphicotylus*, as it is wide and with a convex lateral maxilla projection over the first five maxillary teeth, rather than to *Hulkepholis* which has a thin and straighter skull (Arribas et al., 2019, figure 14). However, the more posterior and closer to the periorbital and skull roof region, the more similar to *Hulkepholis* the shape gets. The skull roof at the

orbit region expands posterolaterally, and the palpebral and postorbital rise laterodorsally over the skull roof, with the frontal in a lower level (character 115 = 1), like *Hulkepholis willetti* (Salisbury and Naish, 2011), rather than having subparallel margins with the periorbital region overall the same level in the skull table as in *Goniopholis* (character 115 = 0) (Andrade et al., 2011). Moreover, the subparallel margins of the nasals are more like that of the North American goniopholidid *Amphicotylus* (character 76 = 1), rather than to the European goniopholidids *Hulkepholis* or *Goniopholis* (character 76 = 0) where these margins are more convex laterally.

Even though the medial borders of the supratemporal fossae are incomplete, most of the left supratemporal fossa is preserved and it allows to compare it with other taxa. The medial border of the left supratemporal fossa is almost straight, similar to the one from *G. simus* (Owen, 1878: plate V) or *H. willetti* (Salisbury and Naish, 2011: text-figure 24.2A) (character 113 = 1), in contrast to the ones from *An. epikrator* (Martin et al., 2016, figure 3) or *G. kiplingi* (Andrade et al., 2011, figure 6) with a more convex shape, displaying a “double concavity” one in front of the other (character 113 = 0).

While the ventral maxillae contribution in the naso-oral fossa is absent (character 68 = 0) in *Ophiussasuchus paimogonectes* gen. et sp. nov. and *Hulkepholis* (Buscalioni et al., 2013; Arribas et al., 2019), the ventral maxillae take part of at least the posterior border of the foramen in *Goniopholis kiplingi* (Andrade et al., 2011) and *Amphicotylus lucasii* (Erickson, 2016) (character 68 = 1). This participation of the maxillae in the foramen has been seen in other *Amphicotylus* that were not included in the matrix of Arribas et al. (2019) such as *Am. milesi* (Yoshida et al., 2021, figure 1C) and *Am. stovalli* (Allen, 2012, figure 3).

Ventrally, in the posterior region of the maxilla, the maxillo-palatine fenestrae (=palatal fenestrae) of ML2776 are present and anteroposteriorly elongated (character 205 = 1) as in *Sunosuchus* (Wu et al., 1996, figure 4B), but not as elongated as in *Calsoyasuchus* (Tykoski et al., 2002), *Eutretraurosuchus* (Pritchard et al., 2013), or *Amphicotylus* (Erickson, 2016). This presence of the #axilla-palatine fenestrae contrasts with the absence of these fenestrae in younger Cretaceous taxa such as *Goniopholis*, *Anteophthalmosuchus*, or *Hulkepholis* (character 205 = 0). From the palatal region of the skull, the development of the nasopharyngeal duct of *Ophiussasuchus paimogonectes* gen. et sp. nov. is morphologically intermediate between the

more basal North American goniopholidids and the younger European goniopholidids. Therefore, in North American Jurassic goniopholidids (*Eutretraurosuchus* and *Amphicotylus*, Figure 5) the primary choana is opened on the anterior palatine region (character 213 = 0) as a long ventrally open duct connected with the opening of the external choana in the pterygoid. However, in *Ophiussasuchus paimogonectes* gen. et sp. nov., there is a reduced palatal opening between the maxillae and the palatines (character 213 = 0), but not completely closed as in the other European goniopholidids (*Goniopholis*, *Hulkepholis* and *Anteophthalmosuchus*) (Andrade et al., 2011; Arribas et al., 2019) (character 213 = 1) being *Ophiussasuchus paimogonectes* gen. et sp. nov. closer in look and shape to *Sunosuchus* (Wu et al., 1996). Also, the secondary choana of *Ophiussasuchus paimogonectes* gen. et sp. nov. displays a wider shape in contrast to the Jurassic North American goniopholidids, in which the choana is longer, thinner, and ventrally opened in most of the duct. Even having a choanal shape closer to the European taxa, it is also different: in *Hulkepholis* and *Anteophthalmosuchus*, the secondary choana is very reduced, and while in *Goniopholis* this opening is bigger, its shape also differs between species of the same genus (e.g., *G. kiplingi* seems to have bigger secondary choana than *G. simus*) (Andrade et al., 2011, supporting information file S1 and figure 4C).

The presence of an anterior opening of the nasopharyngeal duct exposes the vomer between the maxilla and palatine in ML2776, as in older goniopholidid species, such as *Calsoyasuchus* and *Amphicotylus* (character 221 = 2), while it is hidden by the palatal branch of the maxilla in younger species as *Goniopholis* or *Hulkepholis* (character 221 = 0).

Ophiussasuchus paimogonectes gen. et sp. nov. shares with *H. willetti* RIS (RIS = the specimen from Ritstevski et al., 2018), *Eutretraurosuchus delfsi* (AMNH FARB 570) (Pritchard et al., 2013), and *Calsoyasuchus valliceps* (Tykoski et al., 2002) the overall morphology of the palatine process, as a wide anteriorly tapering process that wedges between the palatine rami of the maxilla (character 224 = 1), while in other goniopholidids such as *Goniopholis* and the other *Hulkepholis* species, the morphology of the lateral margins of the palatine process is parallel and flaring anteriorly (character 224 = 2), or in *Anteophthalmosuchus escuchae*, where the palatines display a wide fan-like shape (character 224 = 0). Therefore, the shape of the

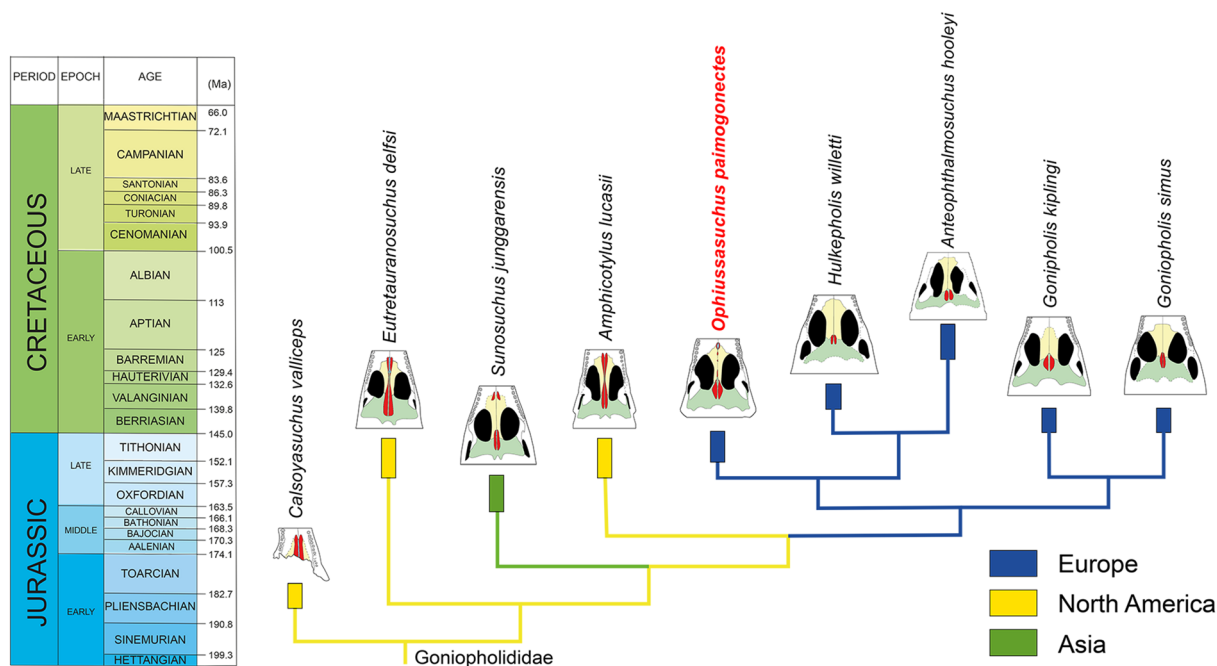


FIGURE 5. Palatal region of some of the goniopholidids, with a simplified cladistic relationship tree between them. The colored areas in the illustrations are the palatines (yellow), the choanae (red), and the pterygoids (green).

palatine process seems to be more truncated anteriorly in younger Cretaceous species (*Hulkepholis*, *Goniopholis*, and *Anteophthalmosuchus*), while in the Jurassic taxa (*Calsoyasuchus* and *Eutretraunosuchus*) the process wedges between the posterior region of the maxillae, as it is also seen in *Ophiussasuchus paimogonectes* gen. et sp. nov.

Moreover, the different number of chambers between the left and right maxillary depressions (four and five, respectively) is for the first time recorded in Goniopholididae. This difference in the number of chambers in the same specimen is an interesting feature, however, whether this asymmetry is a pathology, the result of asymmetric ontogenetic growing, simple erosion or, least likely, an autapomorphy, it is something we cannot determine for now and recovering future specimens could shed light about this issue.

PALAEOBIOGEOGRAPHIC IMPLICATIONS

By the end of the Triassic the break-up of the Laurasian continents, with the opening of the North Atlantic, began to separate Europe from North America. This resulted in a more brackish environment in the Portuguese region (e.g., Lourinhã Fm) rather than the more continental settings observed in the North American continent (Morrison Fm) (Schwarz, 2002; Mateus, 2006). However, faunal

exchange between West Europe and North America by the Late Jurassic has been suggested (Brikiatis, 2016) resulting in similar faunas of dinosaurs (Guillaume et al., 2022; Foster, 2003; Mateus, 2006; Mocho et al., 2019; Rotatori et al., 2020), mammals (Martin, 2001), and crocodylomorphs (Schwarz, 2002).

Brikiatis (2016) also suggests that the separate terrestrial biomes of both continents created good conditions for endemism. This would explain the common genus but different species between both regions, e.g., *Torvosaurus tanneri* Galton and James, 1979 in North America, and *Torvosaurus gurneyi* Hendrickx and Mateus, 2014, in Portugal. Goniopholidids were also common in both regions by the Late Jurassic and Early Cretaceous, however, the putative presence of the genus *Goniopholis* in North America has been renamed as *Amphicotylus* (Mook, 1942; Andrade et al., 2011; Foster, 2020), therefore *Goniopholis* genus is exclusively European.

Although *Ophiussasuchus paimogonectes* gen. et sp. nov. seems closer phylogenetically to the Cretaceous European taxa *Hulkepholis* and *Anteophthalmosuchus*, it is also close geochronologically with the European Jurassic and Cretaceous *Goniopholis*. However, some of the features that make it a new genus and species are plesiomorphic and shared with earlier North American taxa

(*Calsoyasuchus*, *Eutretraurosuchus*, or *Amphicotylus*) such as the absence of perinarial crest and postnarial fossa, the morphology of the nasals, and the presence, shape, and exposure of the maxilla-palatine fenestrae, the choanae and the vomer. These features may indicate that *Ophiussasuchus paimogonectes* gen. et sp. nov. shares traits between the earlier North American taxa and the later European taxa. It possesses a combination of unique synapomorphies and intermediate states of some of the characters (e.g., the partial closure of the nasopharyngeal duct, Figure 5). These traits are not as developed as in more modern goniopholidids, but they also differ from the plesiomorphic state of the clade.

To test this hypothesis, we performed an ancestral state reconstruction analysis (see Appendix 3) of the characters related to the choana and perichoanal structures (characters 205, 213, 221, 224, and 235 in the matrix of Arribas et al., 2019). The ancestral states were reconstructed by the maximum-likelihood-Mk1 method in MES-QUITE (Maddison and Maddison, 2018).

The result of the analyses (see Appendix 3) of the ancestral node between *Ophiussasuchus paimogonectes* gen. et sp. nov., and *Hulkepholis* + *Anteophthalmosuchus* clade shows a high probability (92.8%–98.7%) of presenting the derived state of these characters, as in *Hulkepholis* and *Anteophthalmosuchus*. However, *Ophiussasuchus paimogonectes* gen. et sp. nov. exhibit the primitive condition seen in older American taxa (such as *Calsoyasuchus*, *Amphicotylus*, and *Eutretraurosuchus*) with regard to the shape of the maxillo-palatine fenestra (character 205 = 2), the opened palatal shelves (character 213 = 0), the exposure of the vomer between the maxilla and palatine (character 221 = 2), and a wide palatine wedging anteriorly into the maxilla (character 224 = 1).

In the case of the position of the anterior border of the internal naris, which is located close to the posterior end of the nasopharyngeal duct (character 235 = 2), this feature is shared just with the younger (Early Cretaceous) Asian species *Siamosuchus phuphokensis* Lauprasert, Cuny, Buffetaut, Suteethorn, and Thirakhupt 2007. The ancestral node of these species (*Siamosuchus phuphokensis* and *Ophiussasuchus paimogonectes* gen. et sp. nov.) shows a high probability (99.8%) of presenting the anterior border of the internal naris at mid-duct (character 235 = 1), rather than close to the posterior end (character 235 = 2).

Therefore, these results, along with the current typology of the tree, seem to support a reversion of these characters in *Ophiussasuchus paimogonectes* gen. et sp. nov. to plesiomorphic states within Goniopholididae. However, it is unknown whether these primitive conditions arose due to convergent evolution or by reversion to a plesiomorphic state. Among these characters, the position of the anterior border of the internal naris (character 235) may have experienced convergent evolution with the Asian taxon *Siamosuchus phuphokensis*.

CONCLUSIONS

A new and the most complete skull of crocodylomorph (ML2776) from the Late Jurassic of Lourinhã Fm, was recovered and is here described as a new genus and species, *Ophiussasuchus paimogonectes* gen. et sp. nov.

This new taxon was recovered with a unique combination of 15 synapomorphies. These synapomorphies are a combination of features from both older North American and younger European taxa, such as the shape of the rostrum with a less-projected axe shape compared with Jurassic North American species (*Amphicotylus*) and more similar to Cretaceous taxa, while the nasopharyngeal duct openings are more closed than older species (*Calsoyasuchus* or *Eutretraurosuchus*) but not completely closed as in *Hulkepholis* and *Anteophthalmosuchus*, with which *Ophiussasuchus paimogonectes* gen. et sp. nov. has closer relationships. In addition, ML2776 displays an asymmetrical number of maxillary fossae (four in the left region while five in the right region). However, any hypothesis regarding this asymmetry cannot be contrasted until more specimens are found.

The new taxon *Ophiussasuchus paimogonectes* gen. et sp. nov. increases the already high paleodiversity of crocodylomorphs of the locality. It also supports the hypothesis of a shared fauna between North America (Morrison Fm) and Western Europe (Lourinhã Fm) during the Late Jurassic, as well as the high endemism of Portugal, distinguishing both continents.

DATA ARCHIVING STATEMENT

This published work have been registered in the Morphobank (Project 4730).

ACKNOWLEDGMENTS

Many thanks to HL for finding the specimen, the staff of the Parque dos Dinossauros da Lourinhã. For the preparation work, our thanks to SP, DM, MS, and RS who has become an amazing preparator. To the Museu da Lourinhã staff, CAT, and its board team, namely JR and MM. To CP, a Msc student from Aveiro University, who has done the wonderful illustrations of *Ophiussasuchus pai-mogonectes*. The research was funded by Parque dos Dinossauros da Lourinhã, Museu da Lourinhã,

GeoBioTec grant UIDB/04035/2020 by the Fundação para a Ciência e Tecnologia. EPP was funded by SFRH/BPD/116759/2016 (Fundação para a Ciência e Tecnologia), PID2021-122612OB-I00 (Ministerio de Ciencia e Innovación, Government of Spain) and by a postdoctoral contract María Zambrano (Ministerio de Universidades of the Government of Spain through the Next Generation EU funds of the European Union). VLR was funded by the Fellowship 2021.06877.BD of the Fundação para a Ciência e Tecnologia.

REFERENCES

- Allen, E.R. 2012. Analysis of North American goniopholidid crocodyliforms in a phylogenetic context. PhD Dissertation, University of Iowa. Retrieved from <http://ir.uiowa.edu/etd/3421>
- Andrade, M.B. de. 2009. Solving a century-old mystery: the structure and function of the maxillary depressions of *Goniopholis* (Crocodylomorpha, Neosuchia). *Journal of Vertebrate Paleontology*, 29:54A–55A.
<https://doi.org/10.1080/02724634.2009.10411818>
- Andrade, M.B. de and Hornung, J.J. 2011. A new look into the periorbital morphology of *Goniopholis* (Mesoeucrocodylia: Neosuchia) and related forms. *Journal of Vertebrate Paleontology*, 31:352–368.
<https://doi.org/10.1080/02724634.2011.550353>
- Andrade, M.B. de, Edmonds, R., Benton, M.J., and Schouten, R. 2011. A new Berrisian species of *Goniopholis* (Mesoeucrocodylia, Neosuchia) from England, and a review of the genus. *Zoological Journal of the Linnean Society*, 163:S66–S108.
<https://doi.org/10.1111/j.1096-3642.2011.00709.x>
- Antunes, M.T. 2017. Crocodilos miocênicos de grande tamanho do oeste Europeu: Predação, analogias com “Falsos Gaviais” e Tamanho. *Anuário do Instituto de Geociências*, 40:117–130.
https://doi.org/10.11137/2017_3_117_130
- Arribas, I., Buscalioni, A.D., Royo-Torres, R., Espílez, E., Mampel, L., and Alcalá, L. 2019. A new goniopholidid crocodyliform, *Hulkepholis rori* sp. nov. from the Camarillas formation (early Barremian) in Galve, Spain). *PeerJ*, 7:e7911.
<https://doi.org/10.7717/peerj.7911>
- Benton, M.J. and Clark, J.M. 1988. Archosaur phylogeny and the relationships of the Crocodylia. *The Phylogeny and Classification of the Tetrapods*, 1:295–338.
- Bonaparte, J.F. and Mateus, O. 1999. A new diplodocid, *Dinheirosaurus lourinhanensis* gen. et sp. nov., from the Late Jurassic beds of Portugal. *Revista del Museo Argentino de Ciencias Naturales*, 5:13–29.
- Brikiatis, L. 2016. Late Mesozoic North Atlantic land bridges. *Earth-Science Reviews*, 159:47–57.
<https://doi.org/10.1016/j.earscirev.2016.05.002>
- Buffetaut, E. 1986. Remarks on the anatomy and systematic position of *Sunosuchus miaoi* Young, 1948, a mesosuchian crocodylian from the Mesozoic of Gansu, China. *Neues Jahrbuch für Geologie und Paläontologie-Monatshefte*, 11:641–647.
<https://doi.org/10.1127/njgpm/1986/1986/641>
- Buscalioni, A.D., Alcalá, A.O., Espílez, L., and Mampel, E. 2013. European Goniopholididae from the Early Albian Escucha Formation in Ariño. *Spanish Journal of Palaeontology*, 28:103–122.

- Castanera, D., Silva, B.C., Santos, V.F., Malafaia, E., and Belvedere, M. 2020. Tracking Late Jurassic ornithopods in the Lusitanian Basin of Portugal: ichnotaxonomic implications. *Acta Palaeontologica Polonica*, 65(2):399–412.
<https://doi.org/10.4202/app.00707.2019>
- Cope, E.D. 1875. Check-list of North American Batrachia and Reptilia with a systematic list of the higher groups and an essay on geographical distribution based on the specimens in the U.S. National Museum. *Bulletin of the United States National Museum*, 1:1–104.
- Cope, E.D. 1878. Descriptions of New Extinct Vertebrata from the Upper Tertiary and Dakota Formations. *Bulletin of the United States Geological and Geographical Survey of the Territories*, 4:379–396.
- Costa, F. and Mateus, O. 2019. Dacentrurine stegosaurs (Dinosauria): A new specimen of *Miragaia longicollum* from the Late Jurassic of Portugal resolves taxonomical validity and shows the occurrence of the clade in North America. *PLoS ONE*, 14:e0224263.
<https://doi.org/10.1371/journal.pone.0224263>
- Cunha, P.P., Mateus, O., and Antunes, M.T. 2004. The sedimentology of the Paimogo dinosaur nest site (Portugal, Upper Jurassic). Presented at the 23rd IAS Meeting of Sedimentology.
- Cuny, G., Laojumpon, C., Cheychiw, O., and Lauprasert, K. 2010. Fossil vertebrate remains from Kut Island (Gulf of Thailand, Early Cretaceous). *Cretaceous Research*, 31:415–423.
<https://doi.org/10.1016/j.cretres.2010.05.007>
- Erickson, B.R. 2016. A new skeleton of the Neosuchian crocodyliform *Goniopholis* with new material from the Morrison Formation of Wyoming. *Science Museum of Minnesota Monograph*, 10:1–27.
- Fernandes, A.E., Mateus, O., Bauluz, B., Coimbra, R., Ezquerro, L., Núñez-Lahuerta, C., Suteu, C., and Moreno-Azanza, M. 2021. The Paimogo dinosaur egg clutch revisited: Using one of Portugal's most notable fossils to exhibit the scientific method. *Geoheritage*, 13:66.
<https://doi.org/10.1007/s12371-021-00591-7>
- Foster, J.R. 2003. Paleocological Analysis of the Vertebrate Fauna of the Morrison Formation (Upper Jurassic), Rocky Mountain Region, U.S.A. *New Mexico Museum of Natural History and Science Bulletin*, 23:1–95.
- Foster, J.R. 2020. *Jurassic West: the dinosaurs of the Morrison Formation and their world*. Indiana University Press.
- Galton, P.M. and James, A.L. 1979. A new large theropod dinosaur from the Upper Jurassic of Colorado. *Brigham Young University Geology Studies*, 26:1–12.
- Gervais, P. 1871. Remarques au sujet des Reptiles provenant des calcaires lithographiques de Cerin, dans le Bugey, qui sont conservés au Musée de Lyon. *Comptes Rendus des Séances de l'Académie de Sciences*, 73:603–607.
- Goloboff, P.A. and Catalano, S.A. 2016. TNT version 1.5, including a full implementation of phylogenetic morphometrics. *Cladistics*, 32:221–238.
<https://doi.org/10.1111/cla.12160>
- Goodwin, M.B., Clemens, W.A., Hutchison, J.H., Wood, C.B., Zavada, M.S., Kemp, A., Duffin, C.J., and Schaff, C.R. 1999. Mesozoic continental vertebrates with associated palynostratigraphic dates from the northwestern Ethiopian plateau. *Journal of Vertebrate Paleontology*, 19:728–741.
<https://doi.org/10.1080/02724634.1999.10011185>
- Guillaume, A.R.D., Moreno-Azanza, M., Puértolas-Pascual, E., and Mateus, O. 2020. Palaeobiodiversity of crocodylomorphs from the Lourinhã Formation based on the tooth record: insights into the palaeoecology of the Late Jurassic of Portugal. *Zoological Journal of the Linnean Society*, 189:549–583.
<https://doi.org/10.1093/zoolinnean/zlz112>
- Guillaume, A.R.D., Costa, F., and Mateus, O. 2022. Stegosaur tracks from the Upper Jurassic of Portugal: new occurrences and perspectives. *Ciências da Terra – Earth Sciences Journal*, 20:37–60.
<https://doi.org/10.21695/cterraesj.v20i1.437>
- Hay, O. 1930. *Second Bibliography and Catalogue of the Fossil Vertebrata of North America 2*. Carnegie Institution of Washington, Washington, D.C.
- Hendrickx, C. and Mateus, O. 2014. *Torvosaurus gurneyi* n. sp., the largest terrestrial predator from Europe, and a proposed terminology of the maxilla anatomy in nonavian theropods. *PLoS ONE*, 9:e88905.
<https://doi.org/10.1371/journal.pone.0088905>

- Hill, G. 1989. The sedimentology and lithostratigraphy of the Upper Jurassic Lourinhã Formation, Lusitanian Basin, Portugal. Doctoral dissertation. The Open University, United Kingdom.
- Karl, H.-V., Gröning, E., Brauckmann, C., Schwarz, D., and Knötschke, N. 2006. The Late Jurassic crocodiles of the Langenberg near Oker, Lower Saxony (Germany), and description of related materials (with remarks on the history of quarrying the “Langenberg Limestone” and “Obernkirchen Sandstone”). *Clausthaler Geowissenschaften*, 5:59–77.
- Lauprasert, K., Cuny, G., Buffetaut, E., Suteethorn, V., and Thirakhupt, K. 2007. *Siamosuchus phuphokensis*, a new goniopholidid from the Early Cretaceous (ante-Aptian) of northeastern Thailand. *Bulletin de la Société géologique de France*, 178:201–216.
- Maddison, W.P. and Maddison, D.R. 2018. Mesquite: a modular system for evolutionary analysis. Version 3.40.
<http://mesquiteproject.org>
- Maisch, M.W., Matzke, A.T., and Stöhr, H. 2003. *Sunosuchus* (Archosauria, Crocodyliformes) from the Toutunhe Formation (Middle Jurassic) of the Southern Junggar Basin (Xinjiang, NW-China). *Geobios*, 36:391–400.
[https://doi.org/10.1016/S0016-6995\(03\)00038-X](https://doi.org/10.1016/S0016-6995(03)00038-X)
- Malafaia, E., Mocho, P., Escaso, F., Dantas, P., and Ortega, F. 2019. Carcharodontosaurian remains (Dinosauria, Theropoda) from the Upper Jurassic of Portugal. *Journal of Paleontology*, 93:157–172.
<https://doi.org/10.1017/jpa.2018.47>
- Manuppella, G., Antunes, M.T., Pais, J., Ramalho, M., and Rey, J. 1999. Notícia explicativa da folha 30-A (Lourinhã) da Carta Geológica de Portugal. Esc. 1/50 000. Instituto Geológico e Mineiro.
- Martin, J.E. and Buffetaut, E. 2012. The maxillary depression of Pholidosauridae: An anatomical study. *Journal of Vertebrate Paleontology*, 32:1442–1446.
<https://doi.org/10.1080/02724634.2012.697504>
- Martin, J.E., Delfino, M., and Smith, T. 2016. Osteology and affinities of Dollo’s goniopholidid (Mesoeucrocodylia) from the Early Cretaceous of Bernissart, Belgium. *Journal of Vertebrate Paleontology*, 36:e11534.
<https://doi.org/10.1080/02724634.2016.1222534>
- Martin, T. 2001. Mammalian fauna of the Late Jurassic Guimarota ecosystem. *Publicación Electrónica de la Asociación Paleontológica Argentina*, 7:123–126.
- Martinius, A.W. and Gowland, S. 2011. Tide?influenced fluvial bedforms and tidal bore deposits (late Jurassic Lourinhã Formation, Lusitanian Basin, Western Portugal). *Sedimentology*, 58:285–324.
- Mateus, I., Mateus, H., Antunes, M.T., Mateus, O., Taquet, P., Ribeiro, V., and Manuppella, G. 1998. Upper Jurassic theropod dinosaur embryos from Lourinhã (Portugal). *Memórias da Academia das Ciências de Lisboa*, 37:9.
- Mateus, O. 2006. Late Jurassic dinosaurs from the Morrison Formation (USA), the Lourinhã and Alcobaça formations (Portugal), and the Tendaguru Beds (Tanzania): a comparison. *New Mexico Museum of Natural History and Science Bulletin*, 36:223–231.
- Mateus, O. and Milàn, J. 2010. Crocodyle tracks and traces. *New Mexico Museum of Natural History and Science Bulletin*, 51:83–87.
- Mateus, O. and Estraviz-López, D. 2022. A new theropod dinosaur from the Early Cretaceous (Barremian) of Cabo Espichel, Portugal: Implications for spinosaurid evolution. *PLoS ONE*, 17:e0262614.
<https://doi.org/10.1371/journal.pone.0262614>
- Mateus, O., Dinis, J., and Cunha, P.P. 2017. The Lourinhã Formation: the Upper Jurassic to lower most Cretaceous of the Lusitanian Basin, Portugal—landscapes where dinosaurs walked. *Ciências da Terra – Earth Sciences Journal*, 19:75–97.
- Mateus, O., Puértolas-Pascual, E., and Callapez, P.M. 2019. A new eusuchian crocodylomorph from the Cenomanian (Late Cretaceous) of Portugal reveals novel implications on the origin of Crocodylia. *Zoological Journal of the Linnean Society*, 186(2):501–528.
<https://doi.org/10.1093/zoolinnean/zly064>
- Mocho, P., Royo-Torres, R., Escaso, F., Malafaia, E., de Miguel Chaves, C., Narváez, I., Pérez-García, A., Pimentel, N., Silva, B.C., and Ortega, F. 2017a. Upper Jurassic sauropod record in the Lusitanian Basin (Portugal): Geographical and lithostratigraphical distribution. *Palaeontologia Electronica*, 20.2.27A:1–50.
<https://doi.org/10.26879/662>

- Mocho, P., Royo-Torres, R., Malafaia, E., Escaso, F., Narváez, I., and Ortega, F. 2017b. New data on Late Jurassic sauropods of central and northern sectors of the Bombarral Sub-basin (Lusitanian Basin, Portugal). *Historical Biology*, 29(2):151–169.
<https://doi.org/10.1080/08912963.2015.1137912>
- Mocho, P., Royo-Torres, R., and Ortega, F. 2019. A new macronarian sauropod from the Upper Jurassic of Portugal. *Journal of Vertebrate Paleontology*, 39:e1578782.
<https://doi.org/10.1080/02724634.2019.1578782>
- Mook, C.C. 1921. Individual and age variation in the skulls of Recent Crocodylia. *Bulletin of the American Museum of Natural History*, 44:51–66.
- Mook, C.C. 1942. Skull characters of *Amphicotylus lucasii* Cope. *American Museum Novitates*, 1165:8.
- Mook, C.C. 1964. New species of *Goniopholis* from the Morrison of Oklahoma. *Oklahoma Geology Notes*, 24:283–287.
- Myers, T.S., Tabor, N.J., Jacobs, L.L., and Mateus, O. 2012. Estimating soil pCO₂ using paleosol carbonates: implications for the relationship between primary productivity and faunal richness in ancient terrestrial ecosystems. *Paleobiology*, 38:585–604.
<https://doi.org/10.1666/11005.1>
- Ortega, F., Escaso, F., Gasulla, J.M., Dantas, P., and Sanz, J.L. 2006. Dinosaurios de la Península Ibérica. *Estudios Geológicos*, 62:219–240.
- Owen, R. 1878. Monograph on the fossil Reptilia of the Wealden and Purbeck Formations – Crocodylia (*Goniopholis*, *Pterosuchus*, and *Suchosaurus*). *Palaeontographical Society Monograph*, 7:1–15.
- Pol, D. and Gasparini, Z. 2009. Skull anatomy of *Dakosaurus andiniensis* (Thalattosuchia: Crocodylomorpha) and the phylogenetic position of Thalattosuchia. *Journal of Systematic Palaeontology*, 7:163–197.
<https://doi.org/10.1017/S1477201908002605>
- Pritchard, A.C., Turner, A.H., Allen, E.R., and Norell, A. 2013. Osteology of a North American goniopholidid (*Eutretauranosuchus delfsi*) and palate evolution in Neosuchia. *American Museum Novitates*, 3783:1–56.
- Puértolas-Pascual, E. and Mateus, O. 2020. A three-dimensional skeleton of Goniopholididae from the Late Jurassic of Portugal: implications for the Crocodylomorpha bracing system. *Zoological Journal of the Linnean Society*, 189:521–548.
<https://doi.org/10.1093/zoolinnean/zlz102>
- Puértolas, E., Canudo, J.I., and Cruzado-Caballero, P. 2011. A New Crocodylian from the Late Maastrichtian of Spain: Implications for the Initial Radiation of Crocodyloids. *PLoS ONE*, 6:e20011.
<https://doi.org/10.1371/journal.pone.0020011>
- Puértolas-Pascual, E., Canudo, J.I., and Sender, L.M. 2015. New material from a huge specimen of *Anteophthalmosuchus* cf. *escuchae* (Goniopholididae) from the Albian of Andorra (Teruel, Spain): Phylogenetic implications. *Journal of Iberian Geology*, 41:41–56.
https://doi.org/10.5209/rev_JIGE.2015.v41.n1.48654
- Puértolas-Pascual, E., Blanco, A., Brochu, C.A., and Canudo, J.I. 2016. Review of the Late Cretaceous-Early Paleogene crocodylomorphs of Europe: extinction patterns across the K-PG boundary. *Cretaceous Research*, 57:565–590.
<https://doi.org/10.1016/j.cretres.2015.08.002>
- Ribeiro, V., Mateus, O., Holwerda, F., Araújo, R., and Castanhinha, R. 2014. Two new theropod egg sites from the Late Jurassic Lourinhã Formation, Portugal. *Historical Biology*, 26:206–217.
<https://doi.org/10.1080/08912963.2013.807254>
- Ristevski, J., Young, M.T., Andrade, M.B. de, and Hastings, A.K. 2018. A new species of *Anteophthalmosuchus* (Crocodylomorpha, Goniopholididae) from the Lower Cretaceous of the Isle of Wight, United Kingdom, and a review of the genus. *Cretaceous Research*, 84:340–383.
<https://doi.org/10.1016/j.cretres.2017.11.008>
- Rotatori, F.M., Moreno-Azanza, M., and Mateus, O. 2020. New information on ornithopod dinosaurs from the Late Jurassic of Portugal. *Acta Palaeontologica Polonica*, 65(1):35–57.
<https://doi.org/10.4202/APP.00661.2019>

- Rotatori, F.M., Moreno-Azanza, M., and Mateus, O. 2022. Reappraisal and new material of the holotype of *Draconyx loureiroi* (Ornithischia: Iguanodontia) provide insights on the tempo and modo of evolution of thumb-spiked dinosaurs. *Zoological Journal of the Linnean Society*, 195(1):125–156.
<https://doi.org/10.1093/zoolinnean/zlab113>
- Russo, J., Mateus, O., Balbino, A., and Marzola, M. 2014. Crocodylomorph eggs and eggshells from the Lourinhã Fm. (Upper Jurassic), Portugal. *Comunicações Geológicas*, 101:563–566.
- Salisbury, S.W. and Naish, D. 2011. Crocodylians, p. 305–369. In Batten, D. and Lane, P.D. (eds.), *English Wealden Fossils*. Palaeontological Association, Aberystwyth.
- Salisbury, S.W., Willis, P.M.A., Peitz, S., and Sander, P.M. 1999. The crocodylian *Goniopholis simus* from the Lower Cretaceous of North-Western Germany. *Special Papers in Palaeontology*, 60:121–148.
- Sauvage, H.E. 1897–1898. Vertébrés fossiles du Portugal. Contribution à l'étude des poissons et des reptiles du Jurassique et du Crétacé. *Mémoires de la Direction de Travaux Géologiques du Portugal*, 46.
- Schwarz, D. 2002. A new species of *Goniopholis* from the Upper Jurassic of Portugal. *Palaeontology*, 45:185–208.
<https://doi.org/10.1111/1475-4983.00233>
- Schwarz, D. and Fechner, R. 2004. *Lusitanisuchus*, a new generic name for *Lisboasaurus mitracostatus* (Crocodylomorpha: Mesoeucrocodylia), with a description of new remains from the Upper Jurassic (Kimmeridgian) and Lower Cretaceous (Berriasian) of Portugal. *Canadian Journal of Earth Sciences*, 41:1259–1271.
<https://doi.org/10.1139/E04-059>
- Schwarz, D. and Salisbury, S.W. 2005. A new species of *Theriosuchus* (Atoposauridae, Crocodylomorpha) from the Late Jurassic (Kimmeridgian) of Guimarota, Portugal. *Geobios*, 38:779–802.
<https://doi.org/10.1016/j.geobios.2004.04.005>
- Schwarz, D., Raddatz, M., and Wings, O. 2017. *Knoetschkesuchus langenbergensis* gen. nov. sp. nov., a new atoposaurid crocodyliform from the Upper Jurassic Langenberg Quarry (Lower Saxony, northwestern Germany), and its relationships to *Theriosuchus*. *PLoS ONE*, 12:e0160617.
<https://doi.org/10.1371/journal.pone.0160617>
- Sereno, P.C., Larsson, H.C.E., Sidor, C.A., and Gado, B. 2001. The Giant Crocodyliform *Sarcosuchus* from the Cretaceous of Africa. *Science*, 294:1516–1519.
<https://doi.org/10.1126/science.1066521>
- Sharpe, D. 1850. On the Secondary District of Portugal which lies on the North of the Tagus. *Quarterly Journal of the Geological Society*, 6:135–201.
<https://doi.org/10.1144/GSL.JGS.1850.006.01-02.18>
- Smith, D.K., Allen, E.R., Sanders, R.K., and Stadtman, K.L. 2010. A New Specimen of *Eutretauranosuchus* (Crocodyliformes; Goniopholididae) from Dry Mesa, Colorado. *Journal of Vertebrate Paleontology*, 30:1466–1477.
<https://doi.org/10.1080/02724634.2010.501434>
- Sullivan, R.M. and Lucas, S.G. 2003. *Brachychampsia montana* Gilmore (Crocodylia, Alligatoroidea) from the Kirtland Formation (Upper Campanian), San Juan Basin, New Mexico. *Journal of Vertebrate Paleontology*, 23:832–841.
<https://doi.org/10.1671/A1082-8>
- Taylor, A.M., Gowland, S., Leary, S., Keogh, K.J., and Martinius, A.W. 2014. Stratigraphical correlation of the Late Jurassic Lourinhã Formation in the Consolação Sub-basin (Lusitanian Basin), Portugal. *Geological Journal*, 49:143–162.
- Tykoski, R.S., Rowe, T.B., Ketcham, R.A., and Colbert, M.W. 2002. *Calsoyasuchus valliceps*, a new crocodyliform from the Early Jurassic Kayenta Formation of Arizona. *Journal of Vertebrate Paleontology*, 22:593–611.
[https://doi.org/10.1671/0272-4634\(2002\)022\[0593:CVANCF\]2.0.CO;2](https://doi.org/10.1671/0272-4634(2002)022[0593:CVANCF]2.0.CO;2)
- van Hinsbergen, D.J.J., de Groot, L.V., van Schaik, S.J., Spakman, W., Bijl, P.K., Sluijs, A., Langereis, C.G., and Brinkhuis, H. 2015. A Paleolatitude Calculator for Paleoclimate Studies. *PLoS ONE*, 10:e0126946.
<https://doi.org/10.1371/journal.pone.0126946>

- Walker, A.D. 1970. A revision of the Jurassic reptile *Hallopus victor* (Marsh), with remarks on the classification of crocodiles. *Philosophical Transactions of the Royal Society of London B, Biological Sciences*, 257:323–372.
- Whetstone, K. and Whybrow, P. 1983. A “cursorial” crocodylian from the Triassic of Lesotho (Basutoland), southern Africa. *Occasional Papers of the University of Kansas Museum of Natural History*, 106:1–37.
- Wiman, C. 1932. *Goniopholis kirtlandicus* n. sp. aus der oberen Kreide in New Mexico. *Bulletin of the Geological Institution of the University of Uppsala*, 23:181–189.
- Wu, X.-C., Brinkman, D.B., and Russell, A.P. 1996. *Sunosuchus junggarensis* sp. nov. (Archosauria: Crocodyliformes) from the Upper Jurassic of Xinjiang, People’s Republic of China. *Canadian Journal of Earth Sciences*, 33:606–630.
- Yoshida, J., Hori, A., Kobayashi, Y., Ryan, M.J., Takakuwa, Y., and Hasegawa, Y. 2021. A new goniopholidid from the Upper Jurassic Morrison Formation, USA: novel insight into aquatic adaptation toward modern crocodylians. *Royal Society Open Science*, 8:210320. <https://doi.org/10.1098/rsos.210320>
- Young, C.C. 1948. Fossil crocodiles in China, with notes on dinosaurian remains associated with the Kansu crocodiles. *Bulletin of the Geological Society of China*, 28:255–288.
- Young, M.T., Bell, M.A., Andrade, M.B. de, and Brusatte, S.L. 2011. Body size estimation and evolution in metriorhynchid crocodylomorphs: Implications for species diversification and niche partitioning. *Zoological Journal of the Linnean Society*, 163:1199–1216. <https://doi.org/10.1111/j.1096-3642.2011.00734.x>
- Young, M.T., Hua, S., Steel, L., Foffa, D., Brusatte, S.L., Thüring, S., Mateus, O., Ruiz-Omeñaca, J.I., Havlik, P., Lepage, Y., and Andrade, M.B. de. 2014. Revision of the Late Jurassic teleosaurid genus *Machimosaurus* (Crocodylomorpha, Thalattosuchia). *Royal Society Open Science*, 1:e140222. <https://doi.org/10.1098/rsos.140222>

APPENDICES

APPENDIX 1

TABLE S1. Dimensions and measurements of the holotype skull of *Ophiussasuchus paimogonensis* gen. et sp. nov. p = preserved; e = estimated.

Measurements of the skull	cm
1. Skull, maximum length (from anterior end of premaxilla to quadrate condyle).	37.94
2. Skull, medial length (from anterior end of premaxilla to parietal).	~ 29.2
3. Skull, maximum medial length (from anterior end of premaxilla to supraoccipital).	?
4. Skull, length of the skull table (along the dorsal midline).	34.97
5. Skull, width of the skull table (between posterior end of the squamosals).	7.63 // (e)15.26
6. Skull, width of the skull table (between anterior margin of the supratemporal fenestrae).	11.19
7. Skull, maximum width (between quadrate condyles).	(e)13.49x2 = 27.98
8. Skull, minimum width (at the level of preserved premaxillary tooth).	3.15 (middle) / 6.3 (total)
9. Skull, width at the level of postorbital bar.	13.53
10. Snout, maximum width (at the level of the anterior end of the orbits).	5.49
11. Snout, minimum width (at the level of the premaxillary-maxillary suture).	3.3 (middle) / 6.6 (total)
12. Snout, length (from anterior end of premaxilla to the anterior level of the orbits).	19.64
13. Interorbital, minimum width (in the frontal).	(e)7.41
14. Frontal, width of the anterior process at the anterior margin of the orbits.	2.33
15. Supratemporal fenestra, anteroposterior length.	~ 3.99
16. Supratemporal fenestra, lateromedial width.	3.6
17. Infratemporal fenestra, anteroposterior length.	4.97
18. Infratemporal fenestra, lateromedial width.	2.98
19. Parietal, minimum interfenestral width.	1.1 // (e)2.2
20. Frontal, total length.	10.7
21. Naris, length.	2.06
22. Naris, width.	1.27
23. Quadrate, average width.	3.92
24. Pterygoid, width between the distal flank.	9.15
25. Pterygoid, length in the lateral flank.	7.97
26. Choana, length.	7.89
27. Choana, width.	0.53
28. Orbit, length.	4.49
29. Orbit, width.	3.69
30. Suborbital fenestra, anteroposterior length.	9.98
31. Suborbital fenestra, maximum transverse width.	5.25
32. Jugal, maximum length.	13.98
33. Orbital ramus of the Jugal, thick in the middle.	3.05
34. Orbital ramus of the Jugal, length (up to postorbital bar).	6.91

Measurements of the skull	cm
35. Jugal, infratemporal bar length (from postorbital bar).	5.98
36. Jugal, average thickness of infratemporal bar.	1.2
37. Jugal, average width of infratemporal bar.	1.41
38. Postorbital bar, maximum anteroposterior diameter.	2
39. Postorbital bar, minimum anteroposterior diameter.	1.03
40. Foramen magnum, maximum transverse width.	?
41. Foramen magnum, maximum dorsoventral thickness.	?
42. Premaxilla, maximum width.	3.96+3.75 (mid) / 7.5 (tot)
43. Postsnout length to the supraoccipital.	~ 9.71
44. Postsnout length to the quadrate condyle.	~17.26
45. Width between the fifth maxillary teeth.	6.03 / (p)11.04 / (e)12.06
46. Number of maxillary alveoli.	18
47. Number of premaxillary alveoli.	5

TABLE S2. Ratios of the holotype skull of *Ophiussasuchus paimogonensis* gen. et sp. nov.

Ratios of the skull		%
1. Snout length/Medial Skull length	19.64/29.2	0.6726
2. Snout length/Maximum medial Skull length	19.64/?	?
3. Snout, minimum width/Snout, maximum width	3.3/5.49	0.60109
4. Snout, minimum width/Snout, maximum width	6.6/10.98	0.60109
5. Width between the fifth maxillary teeth/Skull, maximum width	12.06/13.53	0.8913
6. Snout length/Postsnout length to the supraoccipital	19.64/9.71	2.0226
7. Snout length/Postsnout length to the quadrate condyle	19.64/17.26	1.13789
8. Snout, minimum width/Premaxilla, maximum width	3.3/3.96	0.83333
9. Premaxilla, maximum width/Skull, maximum width	3.96/27.98	0.141529
10. Naris, width/Premaxilla, maximum width	1.27/3.96	0.320707
11. Supratemporal fenestra length /Orbit length	3.99/4.49	0.88864
12. Infratemporal fenestra length /Supratemporal fenestra length.	4.97/3.99	1.24561
13. Parietal, minimum interfenestral width/Interorbital, minimum width.	2.2/7.41	0.29689
14. Frontal, width of the anterior process at the anterior margin of the orbits/ Interorbital, minimum width.	2.33/7.41	0.314439
15. Width of the skull table (between the anterior margin of the supratemporal fenestra)/Skull, maximum width	11.19/27.98	0.399928

APPENDIX 2

The character 159 (Orbits, presence of sclerotic ring) was recoded as 0, absent. In Pritchard et al. (2013), figures 4 and 6 there is no presence of sclerotic ring, neither in the block (Pritchard et al., 2013, figure 1) were the skull was embedded in.

The character 195 (Postorbital bar, inclination in anterior view) was recoded as 0, the postorbital bar is vertical (Pritchard et al., 2013, figure 5C).

The character 204 (Quadratojugal, extension of anterodorsal ramus) was recoded as 0, as quadratojugal reaching the dorsal angle of intratemporal fenestra. The quadratojugal is broken, as it is depicted in the Pritchard et al. (2013), figure 5C, missing the uppermost region. However, the state 1 of the character implies that the quadrate participates in the infratemporal fenestra, and even though the quadrate is also broken in its uppermost region, the quadratojugal is dorsally projected and making part of, at least, the lower half of this fenestra. So, as in other goniopholidids such as *Ophiussasuchus paimogonectes* gen. et sp. nov., *Anteophthalmosuchus escuchae* or *Hulkepholis plotos* (Buscalioni et al., 2013), we coded similar here.

The character 211 (Palate, presence of contact between ventral rami of the maxillae) was recoded as 1, with the ventral rami of the maxilla meeting at medial line and forming a secondary bony palate.

The character 209 (presence of the parachoanal fossae) was coded as state 1, present. However, this character has been stayed that appears only in sphagesaurids and baurusuchis (Andrade and Bertini, 2008). We have recoded the character as state "0", absent.

The character 216 (palate, presence of maxillary process to palatine, next to the anterior border of antorbital fenestra) was coded as state "1" and "2", but character state 2 does not exist in the character description. As it seems that it is a mistake, we have removed the character state 2 and keep the state 1, describing the palate as displaying a three-radiated blade anteriorly.

The character 219 (Palate, relative position of the distalmost suture of palatine, at the border of the suborbital fenestra) was recoded as state 0, with the suture in the medial region but at the distal end of the suborbital fenestra.

The character 223 (Palatines, proportional length of anterior process, projecting at maxillary palate (taken from their border at the suborbital fenestra) was recoded as state 0, with the anterior process of the palatines being short with a subequal length and width.

The character 236 (Choanae, position of anterior border of the internal naris relative to pterygoid surface at medial line) was recoded as state 0, with the choana close to the anterior end of the pterygoid, as it can be seen in Pritchard et al. (2013), figure 4B, 5B.

The character 290 (Medial pharyngeal and pharyngotympanic tubes (= "Eustachian tubes"), relation to basioccipital and basisphenoid) is recoded as 1, with the "Eustachian tube" enclosed between the basioccipital and basisphenoid. Pritchard et al. (2013) describe the "Eustachian tube" as the "Eustachian canal", which can be visible in the CT scans (Pritchard et al., 2013, figure 12E) as a distinct tube between the basioccipital and parabasisphenoid.

The character 305 (Otic aperture, morphology of distal margin) was recoded as 0, with the posterior margin not defined, but never invaginated. In the figures from Pritchard et al. (2013) the aperture is not well shown, only CT scans of the posterior region of the skull allowed to describe it. Pritchard et al. (2013) described the otic aperture of *E. delfsi* AMNH FARB 570 as having a similar display to *Goniopholis simus*, so here it has been coded as the in *G. simus*.

For the characters 311 (Posteroventral symphyseal fossa, presence of a single depressed area at the pos-

terior end of symphysis, in ventral view) and 355 (Mandibular glenoid fossa, length relative to width), related with the mandible, they have been recoded as '?', because the characters refer to the medial region of the mandible, and only the lateral region was visible (Pritchard et al., 2013, figures 1, 16).

Something similar happened with the characters 374 (Mid to posterior dentition, presence of pebbled ornamentation on tooth crown surface) and 404 (Symphyseal alveoli 3-4, relative size), related with teeth morphology, but no teeth (character 374) nor the region of the alveoli (character 404) were preserved.

REFERENCES

- Pritchard, A.C., Turner, A.H., Allen, E.R. and Norell, A. 2013. Osteology of a North American goniopholidid (*Eutreptanosuchus delfsi*) and palate evolution in Neosuchia. *American Museum Novitates* 3783:1–56.
- Andrade, M.B., and Bertini, R. J. 2008. A new *Sphagesaurus* (Mesoeucrocodylia: Notosuchia) from the Upper Cretaceous of Monte Alto City (Bauru Group, Brazil), and a revision of the *Sphagesauridae*. *Historical Biology* 20: 101–136. DOI: 10.1080/08912960701642949

APPENDIX 3

FIGURE S1. Likelihood Ancestral State reconstruction of character 205 of the two most parsimonious trees traced over the strict consensus tree, using our matrix based on Arribas et al. (2019).

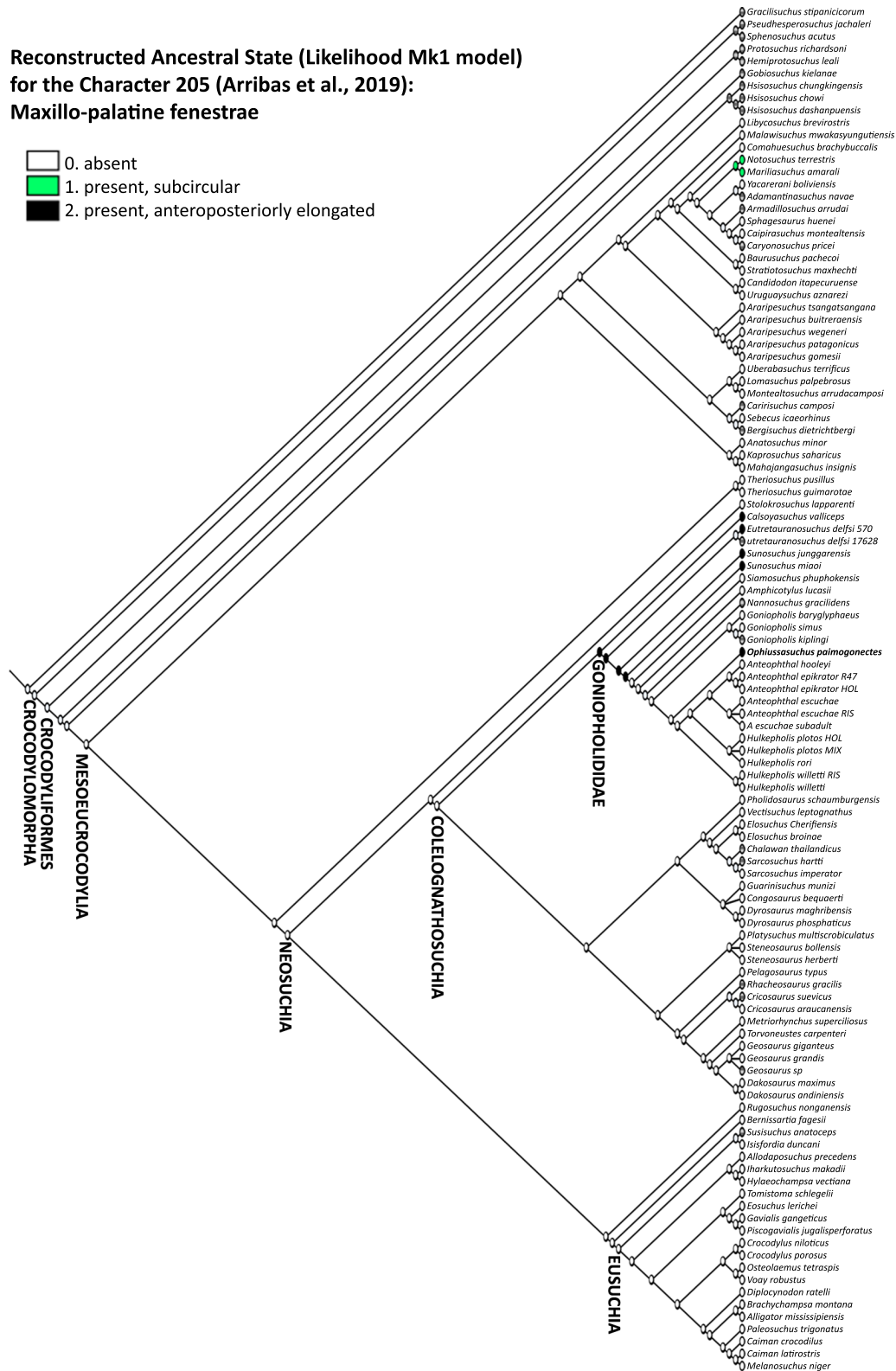


FIGURE S2. Likelihood Ancestral State reconstruction of character 213 of the two most parsimonious trees traced over the strict consensus tree, using our matrix based on Arribas et al. (2019).

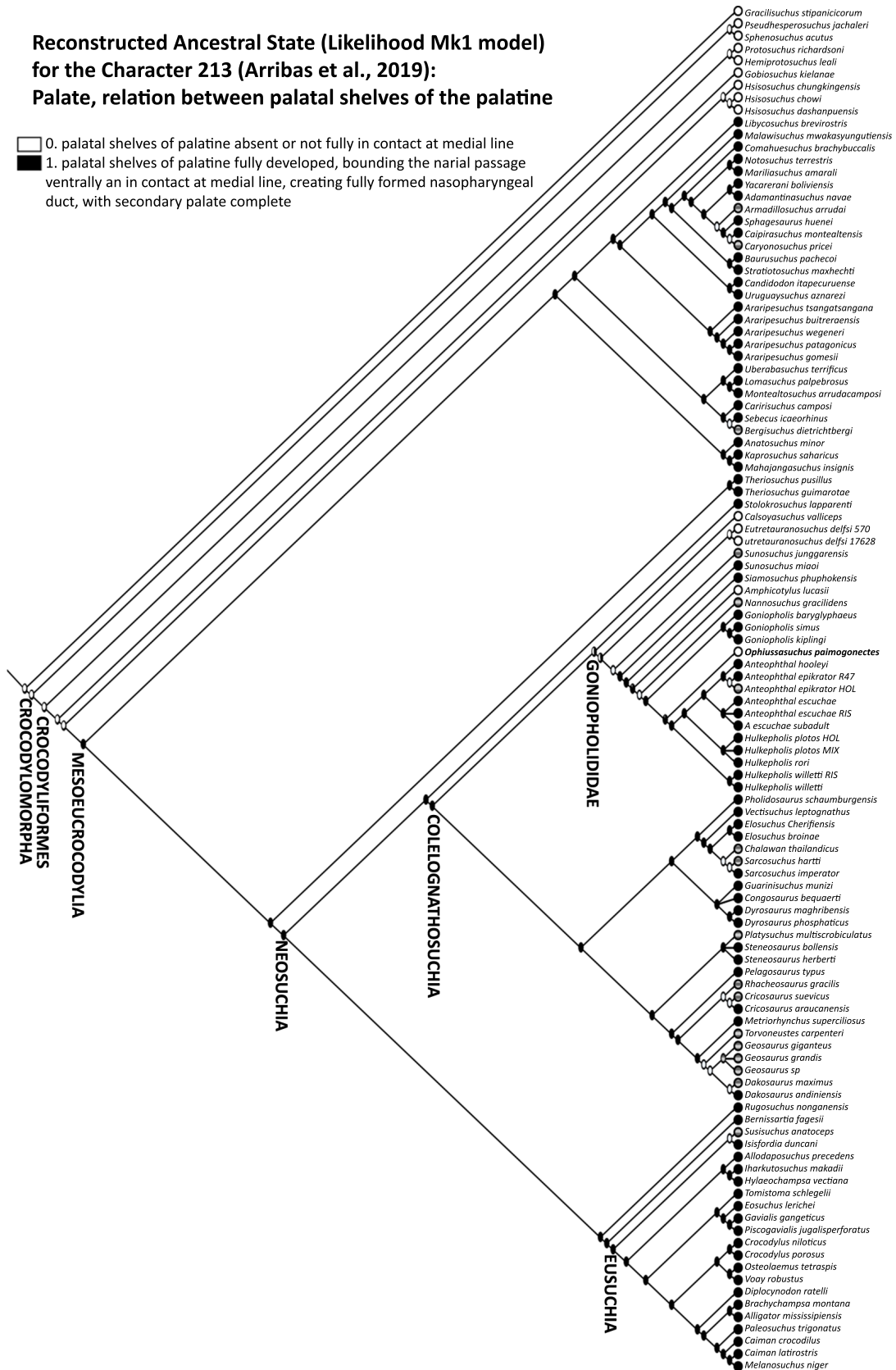


FIGURE S3. Likelihood Ancestral State reconstruction of character 221 of the two most parsimonious trees traced over the strict consensus tree, using our matrix based on Arribas et al. (2019).

**Reconstructed Ancestral State (Likelihood Mk1 model)
for the Character 221 (Arribas et al., 2019):
Vomer, ventral exposure on palate**

- 0. not exposed on palate, hidden by palatal branch of maxillae
- 1. exposed on palate between premaxillae and maxillae
- 2. exposed on palate between maxilla and palatine

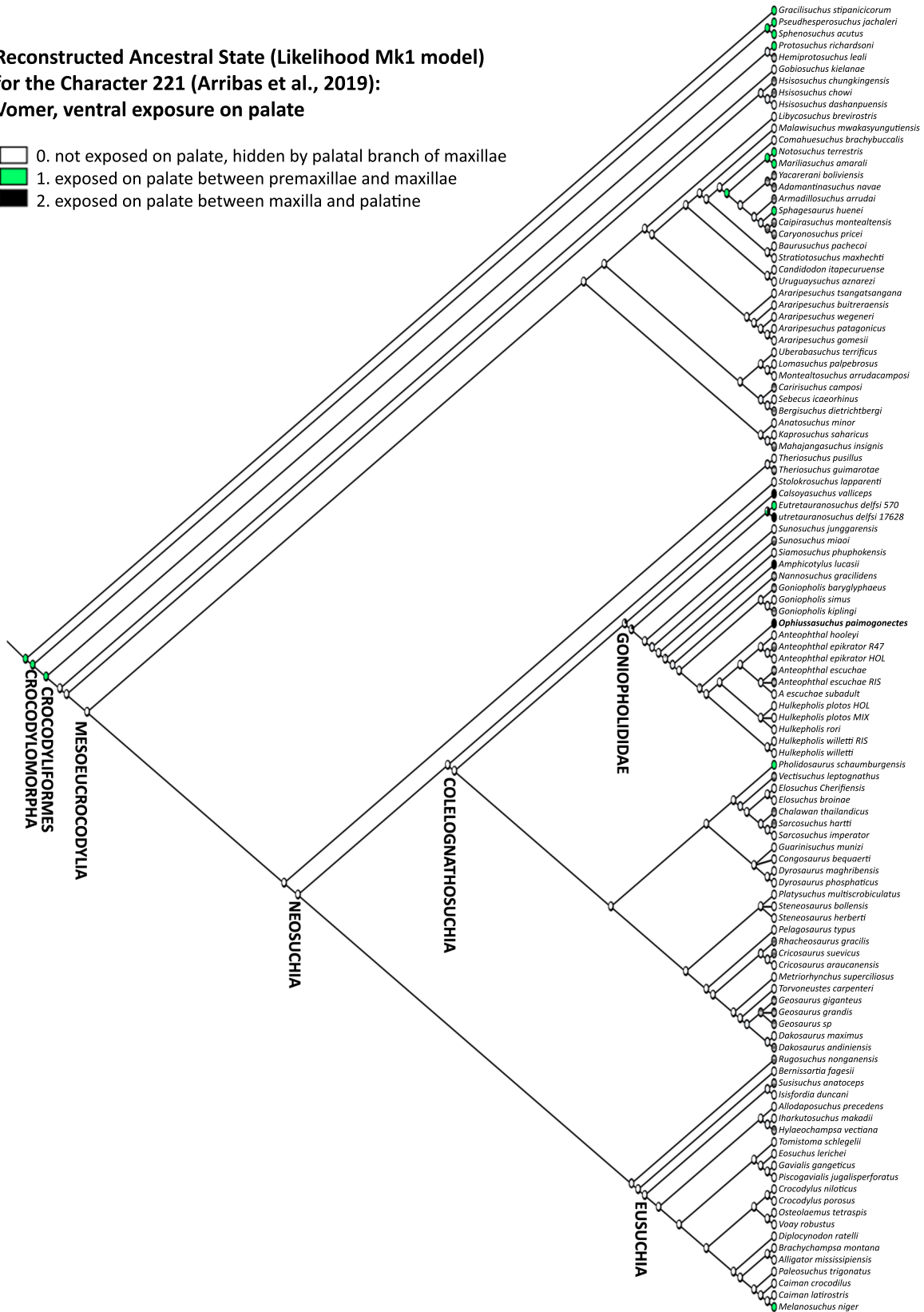


FIGURE S4. Likelihood Ancestral State reconstruction of character 224 of the two most parsimonious trees traced over the strict consensus tree, using our matrix based on Arribas et al. (2019).

**Reconstructed Ancestral State (Likelihood Mk1 model)
for the Character 224 (Arribas et al., 2019):
Palatines, overall morphology of palatine process**

- 0. wide, fan-like
- 1. wide posteriorly and tapering anteriorly, wedging between palatine rami of maxilla
- 2. lateral margins parallel or flaring anteriorly

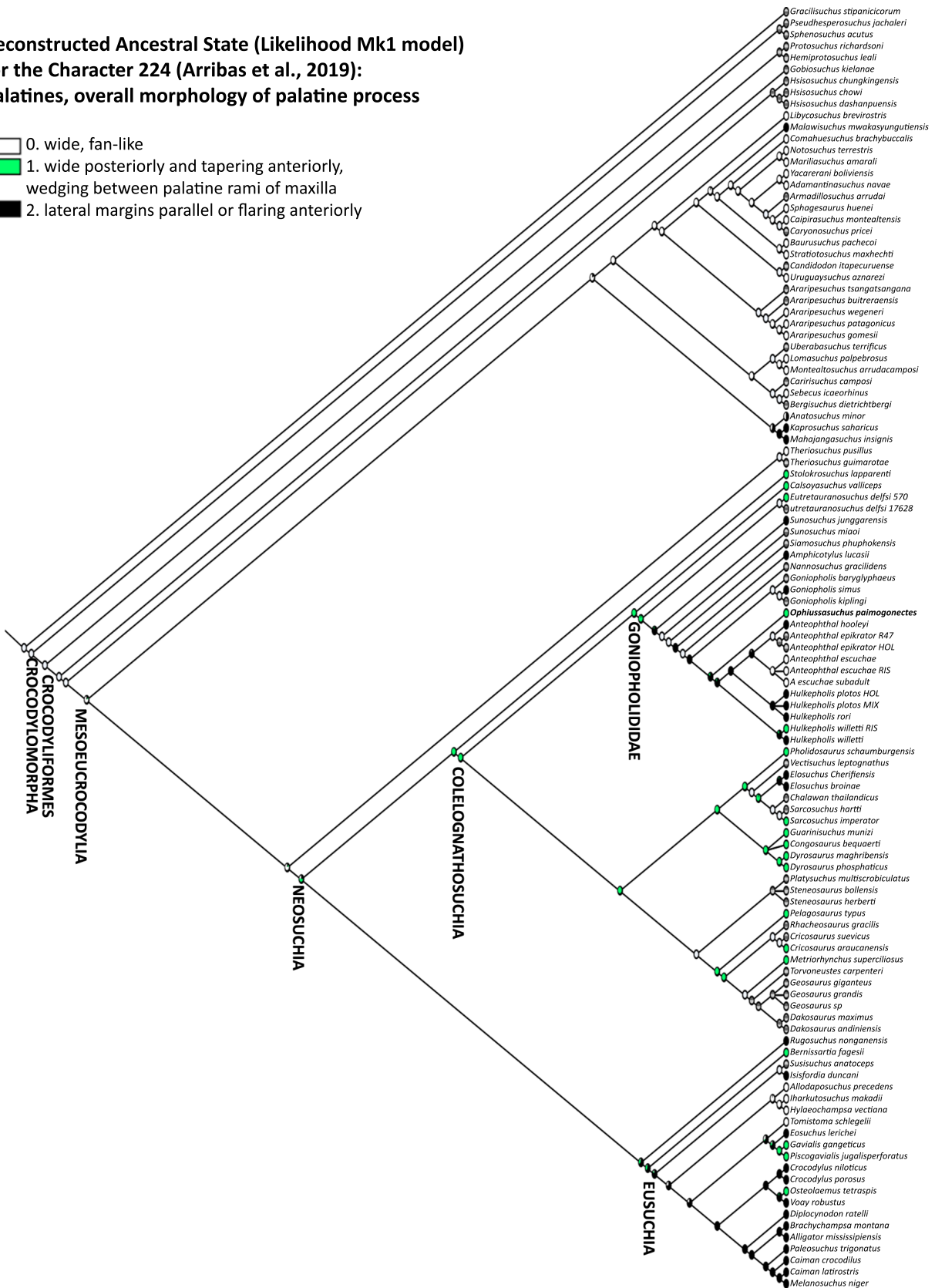


FIGURE S5. Likelihood Ancestral State reconstruction of character 235 of the two most parsimonious trees traced over the strict consensus tree, using our matrix based on Arribas et al. (2019).

